Received: 27 January 2025 | Accepted: 30 December 2025

DOI: 10.1111/2041-210x.70242

Methods in Ecology and Evolution

RESEARCH ARTICLE

As above, so below: A perspective into the application of land-forest monitoring methods for the assessment of marine animal forests

Torcuato Pulido Mantas[1,2] | Camilla Roveta[1,2] | Martina Coppari[1,2] | Cristina Gioia Di Camillo[1,2] | Joaquim Garrabou[3] | Nils Lucas Jacobsen[4] | Marco Palma[5] | Ubaldo Pantaleo[5] | Manuja Promodya Hendawitharana[6,7] | Carlo Cerrano[1,2,8,9]

[1]Dipartimento di Scienze della Vita e dell'Ambiente, Università Politecnica delle Marche, Ancona, Italy; [2]National Biodiversity Future Center (NBFC), Palermo, Italy; [3]Departament de Biologia Marina, Institut de Ciències del Mar (CSIC), Barcelona, Spain; [4]Institute of Natural Sciences, OD Nature, Marine Ecology and Management, Royal Belgian Institute of Natural Sciences, Brussels, Belgium; [5]Underwater Bio-Cartography (UBICA) S.r.l., Genoa, Italy; [6]National Aquatic Resources Research and Development Agency (NARA), Colombo, Sri Lanka; [7]Department of Biology, Ghent University, Ghent, Belgium; [8]Stazione Zoologica di Napoli Anton Dohrn, Naples, Italy and [9]Fano Marine Center, Fano, Italy

Correspondence
Camilla Roveta
Email: c.roveta@staff.univpm.it

Funding information
Mercuria Energy Group Ltd; NextGenerationEU, Grant/Award Number: CN_00000033; Horizon 2020 Framework Programme, Grant/Award Number: 12091; Interreg, Grant/Award Number: 5216

Handling Editor: Yu Ren

Abstract

1. Marine animal forests (MAFs) are benthic ecosystems dominated by vertically structuring filter- and suspension-feeders. As terrestrial forests, they are considered biodiversity hotspots, forming canopies, serving as a refuge, nursery, reproduction and feeding shelters for many species. Until just recently, these habitats have represented a challenge in terms of field work and monitoring activities, especially when approaching medium to large scales. However, thanks to the coupling of emerging techniques, such as machine learning and photogrammetry, the development of cost-effective approaches to assess MAFs might be closer than ever.
2. The main aim of this study is, therefore, to provide an innovative perspective to monitor canopy-forming organisms (CFOs). In the first place, Structure from Motion (SfM) photogrammetry was applied to capture the three-dimensional (3D) features from the surveyed benthic assemblage. Subsequently, similarly to the procedures used in airborne LiDAR surveys of terrestrial forests, the resulting 3D point clouds were further processed in a five-step workflow: (i) point cloud denoising; (ii) classification and filtering of ground points; (iii) *Z*-value normalization to correct substrate irregularity during the height assessment; (iv) individual CFO detection and height assessment; and (v) canopy volume and occupancy quantification.
3. The results obtained with the semi-automated pipeline were compared to manual quantifications of CFO abundance, density and height frequencies derived from point clouds produced for five Mediterranean MAFs. Broad comparability was

found for CFO detection, with an average F_1-score of 0.77 ± 0.12. However, limitations were identified in the estimation of CFO heights, which showed an average value R^2 value of 0.55 ± 0.29. This limitation stemmed from the overall height overestimation in areas with highly irregular substrates.

4. Despite these limitations, the approach presented here marks the first semi-automatic quantitative analysis of MAF canopy structure and represents a crucial step forward in monitoring and managing these endangered habitats, shifting from species/population-level assessment to a more ecologically comprehensive approach for evaluating MAF's integrity.

KEYWORDS
3D, canopy, semi-automated segmentation, SfM-photogrammetry, structural complexity

1 | INTRODUCTION

The ecological and economic importance of terrestrial forests has been acknowledged since early human history (Küster, 2010). These forests do not only provide economic resources, but they also play a key role in global biogeochemical cycles, offering a full spectrum of provisioning, regulating and cultural ecosystem services (Manes et al., 2016; Sacchelli et al., 2021; Sannigrahi et al., 2019). However, it was not until the 18th century that systematic inventories and monitoring programs were established, driven by growing concerns about wood availability and forests' health (FAO, 1948; Innes, 1993). Since then, numerous methods for assessing forest composition and vertical structure have emerged, with recent advancement focusing on automated approaches mainly based on satellite imagery and airborne LiDAR (Borghi et al., 2025; Ferretti, 2013). While these technologies still face some limitations at single-tree level, they offer a significant reduction in cost and time, enabling broader coverage, higher sampling efforts and more robust datasets for long-term landscape management and planning (Fassnacht et al., 2024), building fundamental baselines.

History seems to be repeating itself for their marine analogue, where the development of effective conservation and monitoring plans is taking place after decades of indiscriminate human-driven "deforestation" processes. Marine animal forests (MAFs) are animal-dominated habitats mainly composed of megabenthic long-living sessile filter- and suspension-feeders (e.g. sponges, cnidarians, bryozoans, ascidians), characterized by prominent vertically structuring forms, significantly contributing to the overall seafloor complexity (Cerrano et al., 2010; Orejas et al., 2022; Rossi et al., 2017). When occurring in moderate to high densities they create the so-called canopy effect, similarly to trees in terrestrial ecosystems (Guizien & Ghisalberti, 2017; Lasker et al., 2020, 2025). Their three-dimensional (3D) structure offers a wide range of ecological niches, acting as refuge and feeding grounds for many organisms, and representing essential shelter, spawning and nursery areas for many species of both conservation and economic interest (Gori et al., 2017; Rossi, 2013). Up until today, only emblematic MAFs (i.e., tropical coral reefs) are considered in international management plans, leaving "less charismatic" ones (e.g., sponge beds, gorgonian and hydrozoan forests, bryozoan and tube worm reefs) poorly represented in most marine policies and conservation plans (Orejas et al., 2022). Furthermore, the considerable variation in taxonomy, morphology, life history traits and geographic distribution poses substantial challenges to conservation and management strategies, which, when implemented, are often limited in their effectiveness (Cerrano et al., 2019; Orejas et al., 2022). Therefore, a consistent framework encompassing all MAFs types is needed to provide policymakers with a set of comprehensive tools for their proper conservation, management, monitoring and restoration (Orejas et al., 2022; Rossi, 2013; Rossi et al., 2017, 2022).

Since the last decade, MAFs and marine canopy studies were carried out mainly by scuba diving, mostly applying traditional in situ approaches (e.g., visual/photo/video-sampling, sample collection, among others) (Cerrano et al., 2019; Tsounis et al., 2018; Turner et al., 2017). More recently, the rapid technological development and the appearance of innovative techniques are opening up new possibilities (Rossi et al., 2021), with the emergence of optical methods (e.g., Structure from Motion (SfM) photogrammetry) allowing to obtain accurate 3D reconstructions of benthic ecosystems (Pulido Mantas, Roveta, Calcinai, di Camillo, et al., 2023). SfM-photogrammetry has already been shown to be a suitable approach to investigate the structural complexity both in space and time, being a well-established method in the monitoring toolbox of tropical MAFs (Bayley & Mogg, 2020; Burns et al., 2015; Martínez-Quintana et al., 2023; Palma et al., 2017, 2019; Urbina-Barreto, Chiroleu, et al., 2021; Urbina-Barreto, Garnier, et al., 2021). The great experience acquired in tropical reefs has, in fact, facilitated: (i) the development and implementation of cost-effective fully or semi-automated workflows to reduce post-processing segmentation times of SfM outputs (Remmers et al., 2024; Rossi et al., 2021; Sauder et al., 2024); and (ii) the development of new approaches to measure habitats' functional structural complexity (e.g., shelter capacity, recruitment niches) (González-Rivero et al., 2017; Martínez-Quintana et al., 2023; Torres-Pulliza et al., 2020; Urbina-Barreto,

Chiroleu, et al., 2021). While these new approaches are increasingly being applied to other MAF ecosystems (e.g., soft-coral forests, sponge beds), helping to bridge the gap between "charismatic" and "less charismatic" habitats (de Oliveira et al., 2022; Heres et al., 2024; Marlow et al., 2024; Palma et al., 2018; Prado et al., 2019, 2021; Pulido Mantas et al., 2024; Pulido Mantas, Roveta, Calcinai, Coppari, et al., 2023; Ríos et al., 2020), much work remains to be done.

This study proposes a novel framework for adapting terrestrial forest remote sensing-based approaches to monitor marine ecosystems. By leveraging SfM-photogrammetry and LiDAR-inspired point cloud processing, it bridges methodologies from land-based forestry to MAFs. To this end, Mediterranean gorgonian forests dominated by two species, *Paramuricea clavata* (Risso, 1826) and *Eunicella singularis* (Esper, 1791), were surveyed through SfM-photogrammetry. The height frequencies and densities of canopy-forming organisms (CFOs, *sensu* Smith et al., 2022) were manually quantified from the resulting point clouds. The proposed semi-automatic pipeline was then applied to replicate these measurements, allowing for a comparison between the two methods. Additionally, for the first time, this approach provided a direct estimate of the total canopy volume created by the forest, a crucial ecological characteristic of these habitats, previously estimated by geometric models (Lasker et al., 2025) or indirect proxies such as organisms' density and height frequencies (Bosch et al., 2023; Gambrel & Lasker, 2016).

In summary, despite the limitation faced in directly adapting land-forest methods to their marine counterparts, the approach presented here provides a new methodological perspective aimed at bridging the existing gap in MAFs research. Ultimately, it paves the way for future studies that leverage 3D point cloud-based techniques, which hold significant potential for cost-effective monitoring of changes in the biological structural complexity of vital marine habitats, an often overlooked yet essential aspect in marine ecological research.

2 | MATERIALS AND METHODS

2.1 | Study sites

The imagery for the 3D digital reconstructions of the gorgonian forests was collected in three Mediterranean locations: (i) Cap de Creus Natural Park (Catalan Sea, Spain); (ii) Portofino Marine Protected Area (MPA) (Ligurian Sea, Italy); and (iii) Punta Manara Special Area of Conservation (Ligurian Sea, Italy) (Figure 1). A single site was assessed

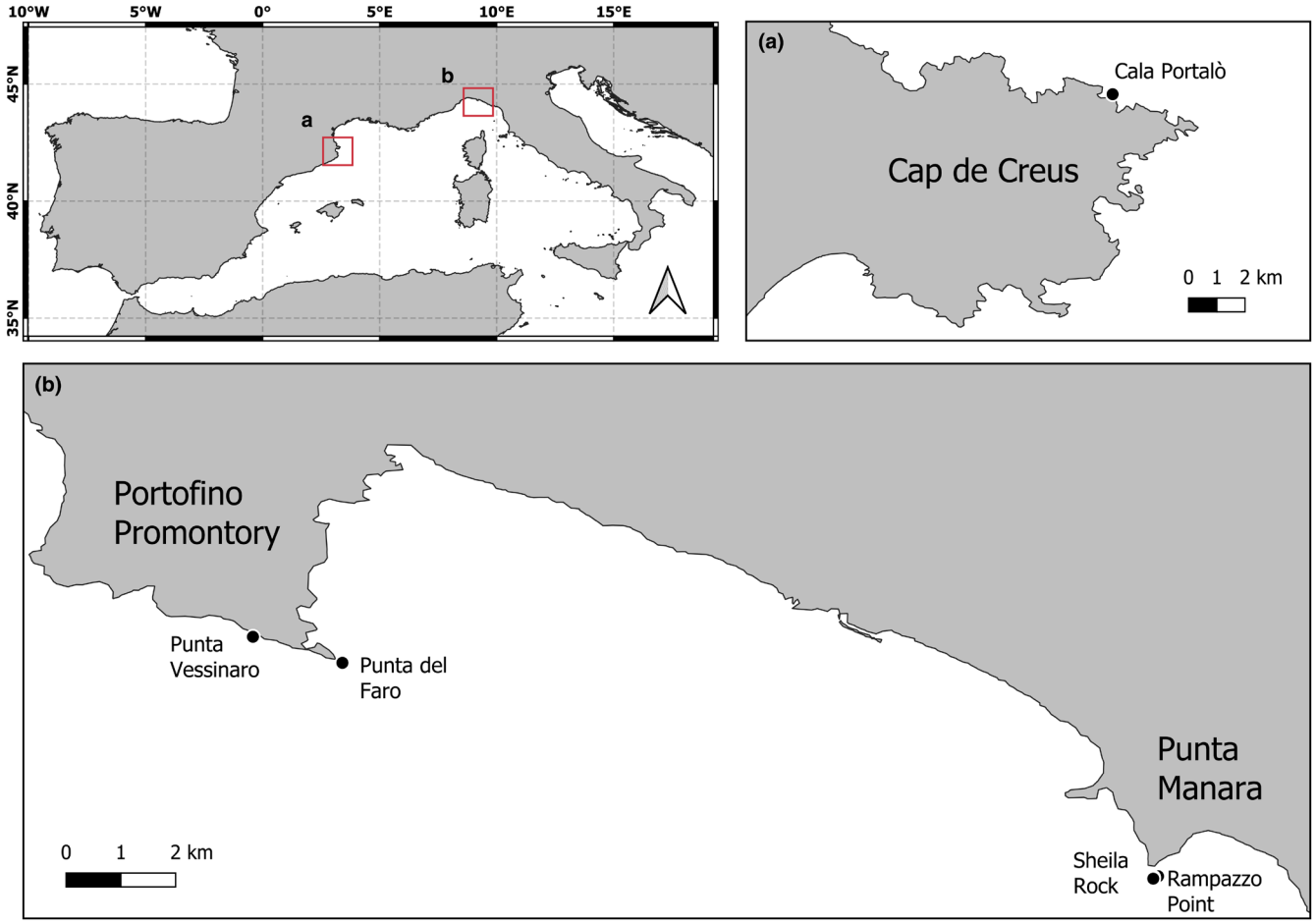

FIGURE 1 Map with the location of the study sites: (a) Cala Portalò in Cap de Creus Natural Park (Spain); (b) Punta del Faro and Punta Vessinaro in Portofino Marine Protected Area (Italy), and Sheila Rock and Rampazzo Point in Punta Manara Special Area of Conservation (Italy).

in Cap de Creus (Cala Portalò) (Figure 1a), while two sites were surveyed in both Portofino MPA (Punta Vessinaro and Punta del Faro) and Punta Manara (Sheila Rock and Rampazzo Point) (Figure 1b).

All sites were selected based on the presence of MAFs, which in the locations of Portofino and Punta Manara were dominated by *Paramuricea clavata*, and in Cala Portalò, in Cap de Creus, by *Eunicella singularis* (Figure 2). Sampling activities were carried out between 20 and 42 m depth (Table S1), in the late summer of 2021 and the spring of 2022 in the framework of two projects: the Interreg MED MPA Engage (Garrabou, Bensoussan, et al., 2022) and the Punta Manara Project, a citizen science initiative developed by Reef Alert Network (https://www.reefalert.org/). Since no invasive sampling technique was applied, no licence or permit was required.

2.2 | Dominant canopy-forming species

The red gorgonian *P. clavata* is an azooxanthellate octocoral, with a colouration varying from purple to yellow (Figure 2a). This species can grow into large fan-shaped colonies (up to 1 m high), usually as wide as tall, with thick branches generally arranged in a single plane, and polyps closely packed together (Carpine & Grasshoff, 1975; Pica et al., 2018). *P. clavata* is recognized for generating highly dense and three-dimensional aggregations, often creating forests, thus increasing the overall habitat complexity and supporting high levels of biodiversity (Ponti et al., 2018).

The white gorgonian *E. singularis* is a zooxanthellate octocoral displaying brownish- or greyish-white colour. The species presents two main depth-dependent morphotypes. The "candlestick" structure typical in shallow environments (Figure 2b) could be related to its symbiosis, reducing self-shading and increasing the photosynthetic surface (Weimbauer & Velimirov, 1998). In deeper waters, *E. singularis* shows more variable branching patterns, colony shapes and a brighter white colouration, due to the lack of the symbiotic algae (Gori et al., 2012; Weinberg, 1976). Conversely to *P. clavata*, *E. singularis* aggregations (< 35 m) usually create smaller canopies due to their different morphology and overall lower densities (Gori et al., 2012).

Due to a synergy of direct (e.g., fishing activities) and indirect (e.g., climate change) human-driven pressures, both species populations are highly threatened and suffering a steep decrease at Mediterranean level (Garrabou, Gómez-Gras, et al., 2022), threatening the integrity and many functions by these CFOs (Gómez-Gras et al., 2021).

2.3 | Photographic sampling

Photogrammetric surveys were performed using four different cameras: (i) a Sony α7 II, (ii) a Sony α7 III, (iii) a Nikon D7000 and (iv) an Olympus TG-5, always equipped with an artificial lighting system composed by a couple of underwater video lights, allowing for a homogeneous lighting of the scene. A more detailed description of the imaging systems and sampling information for each of the surveyed sites is provided in Table S1.

The sampling protocol implemented for all survey operations was based on Palma et al. (2018) and consisted of: (i) the placement of a minimum of three metric references (PVC tubes of 1 m, 0.2 m × 0.2 m quadrats or three-axial references of 0.2 m × 0.2 m × 0.2 m) in the area of interest; (ii) cameras set to time-lapse mode recording two images per second, with the camera system oriented obliquely to the substrate (around 70°) and at an approximate distance of 1–1.5 m; (iii) diving operators following a boustrophedonic pattern (e.g., perpendicular double zigzag path), aiming to capture the full structural complexity of the area from all possible perspectives. Diving operators maintained a moderate speed that could ensure a minimum overlapping of 60% between each pair of consecutive images.

2.4 | Photogrammetric processing and manually extracted CFO derived metrics

Before starting the photogrammetric processing, all media collected were inspected to verify both the quality and the sequential

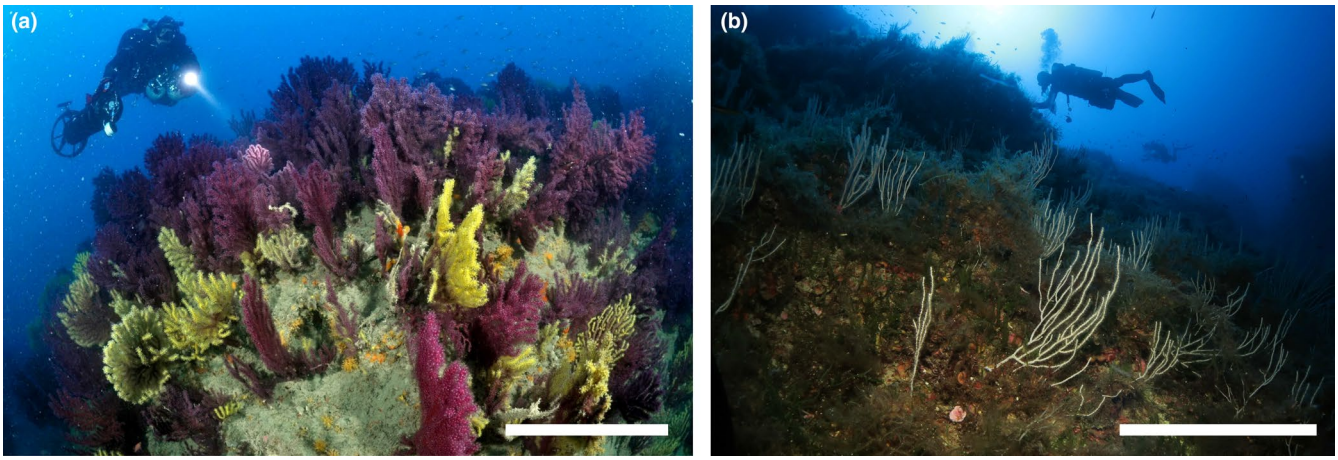

FIGURE 2 Examples of marine animal forests dominated by: (a) *Paramuricea clavata* and (b) *Eunicella singularis*. Scale bars = 50 cm.

overlapping of the imagery. Consecutively, all selected images were imported into Agisoft Metashape v.1.8.3 (Agisoft LLC., St. Petersburg, Russia). Image alignment was carried out using high accuracy generic pair selection settings to generate the point clouds, limiting the tie point limit per Mpx to 4,000 common feature points and the key points identification to 100,000. To scale up the reconstructions, a minimum of 3 metric references were manually detected to generate up to 5 scale bars in the reference settings and specify its dimensions; in addition, to indicate the accuracy of the alignment, root mean square error (RMSE) of the scale bars and check bars was computed (Pulido Mantas, Roveta, Calcinai, Coppari, et al., 2023). A first noise-cleaning step was performed in Metashape in which points holding a confidence below 2 were discarded and not considered in the analysis. Moreover, to standardize the resolution of the study and to reduce the size of the point clouds and later processing times, all dense point clouds were resampled at 1 mm resolution and exported in *.LAS* format at local coordinate system (m) for further analysis. The overall photogrammetric process to generate the 3D point clouds took an average of 6.88 ± 5.07 h of processing time using a Lenovo Legion laptop (Beijing, China) with 32 Gb RAM, an Intel Core i7-9750H 2.60-GHz processor (Intel Corporation, Santa Clara, CA, USA) and a graphic card NVIDIA GeForce RTX 2060 (NVIDIA Corporation, Santa Clara, CA, USA).

Manual height measurement of each CFO was performed in the 3D point clouds by using the *ruler* tool in Metashape. The height was established as the distance between the base of the CFO and the largest ramification, respecting organism perpendicularity to the substrate. To ensure the measurement accuracy, the ruler position was inspected by changing perspective in the 3D environment and repeating the height assessment up to three times to check measurement consistency (Heres et al., 2024). All CFOs were classified at the lowest taxonomic level possible by inspecting the imagery in relation to the dense point cloud colouration. Conversely, the 3D surface of each study site was estimated in Metashape, which was then used to calculate the CFOs' densities by dividing the total number of identified CFOs by the corresponding surveyed area for each site. To do so, (i) firstly, the mesh was generated by the arbitrary 3D surface type based on the point clouds, medium face count and interpolation disabled; (ii) secondly, cleaning the mesh from CFOs and closing the possible holes created by this intermediate step with the tool *close holes* in the mesh toolbox; (iii) and lastly, measuring the surface of the remaining 3D mesh by using the Metashape *measure area and volume* tool (Pulido Mantas, Roveta, Calcinai, Coppari, et al., 2023).

2.5 | Point cloud processing and semi-automated CFO derived metrics

All point clouds calculated in Metashape were imported and processed in R software v.4.3.2. (R Core Team, 2024). A multi-step workflow (Figure 3) was followed using different functions from the *lidR* package (Roussel et al., 2020): (i) point clouds (*.LAS* format) were imported using the *readLAS* function; (ii) secondly, the outliers present in the point cloud were classified using the function *classify_noise* and the *SOR* noise segmentation algorithm, based on Statistical Outliers Removal (Rusu & Cousins, 2011) and removed using the *filter_poi* function; (iii) subsequently, the filtered point cloud was binary segmented (in ground and CFO points) by using the *classify_ground* function and the Cloth Simulation Filtering (CSF) algorithm, which consists of simulating a piece of cloth draped over the reversed point cloud and detect ground points based on the distance between the nodes of the cloth and the inverted point cloud (Zhang et al., 2016); (iv) the point cloud segmentation was followed by a height normalization process to remove the influence of the seafloor on above substrate measurements, to do so the *normalize_height* function using the k-nearest neighbour algorithm with an inverse-distance weighting was applied; (v) finally, CFO's tops were detected by applying the find_*trees* function using the Local Maximum Filter (LMF) algorithm, inspired by Popescu and Wynne (2004). The identified CFO tops were plotted along with the segmented point cloud using the *plot* and *add_treetops3d* functions to visually inspect in a 3D environment the accuracy of the CFO's tops detection. Number and height of each of the detected CFOs by this procedure were extracted for further analysis (e.g. density calculations, height ranges).

In addition, in order to obtain an estimation of the canopy volume created by the ensemble of CFOs, a voxelization process of the classified point cloud was performed, similarly to the approach currently used in terrestrial forests (Hess et al., 2018; Li et al., 2024; Smeds et al., 2025; Weiser et al., 2021). To do so, the points classified as ground were filtered out using the *filter_poi* function, and a voxelization of the remaining point cloud (representing CFOs) was carried out using the *voxelize_points* function. A voxel size of $0.1\,m \times 0.1 \times 0.1\,m$ was chosen as a trade-off value, found to be an optimal value for canopy and visibility analysis in terrestrial forests (Rossi et al., 2022; Zong et al., 2021). Calculating the volume contained by the voxels, it was possible to estimate the "canopy occupation volume" produced by the MAF and after divided by each study site assessed surface was expressed as m^3/m^2. All R code corresponding to the point cloud processing and analysis can be found in Pulido Mantas et al. (2026).

2.6 | Point cloud processing pipeline sensitivity analysis

All three main processing steps of the proposed point cloud pipeline require parametrization, with key attributes likely to be different for the processing of point clouds derived from airborne laser scanning of terrestrial forests and the ones deriving from underwater photogrammetry of MAFs. To optimize the overall pipeline performance, a sensitivity analysis was performed by running many iterations of the main processing steps. Considering the strong influence of slope on ground classification and treetop detection (Graham et al., 2019; Khosravipour et al., 2015; Li

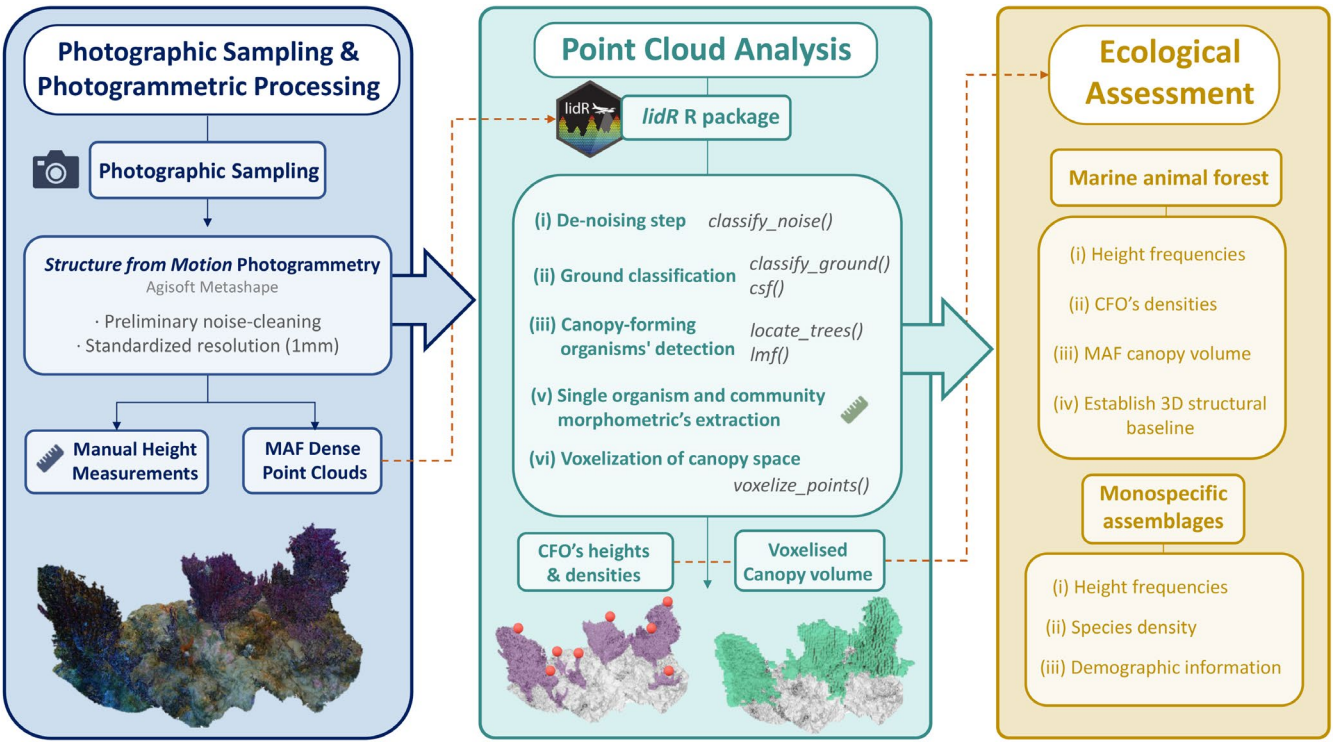

FIGURE 3 Schematic diagram summarizing the different steps of the workflow of the study: Imagery collection and photogrammetric processing, to point cloud post-processing and, finally, morphometric and MAF descriptors extraction and ecological interpretation.

et al., 2025; Meng et al., 2010), four study sites presenting different roughness and slope were selected for this analysis (Punta del Faro, Punta Vessinaro, Shila Rocks and Rampazzo Point). The three processing steps considered for the sensitivity analysis were as follows:

(i) Noise detection, performed by the SOR algorithm (Rusu & Cousins, 2011), which required 2 attributes: *k*, representing the number of points used to calculate the mean distance between k-neighbouring points, and *m*, representing the multiplier used to define the maximum distance at which the points would not be considered noise by the algorithm. Three different parameter combinations were explored (Table 1), and each combination parameter combination was assessed by visually inspecting the segmentation output along with the percentage calculation of outlier points (Table S2).

(ii) Ground classification, carried out using the CSF algorithm (Zhang et al., 2016), which required three attributes: *sloop_smooth*, a post-processing step to reduce errors and the impact of noise when assessing areas with sharp or steep slope, set as *TRUE* following authors' instructions; *cloth_resolution*, the distance between the particles in the simulated cloth, usually set as the average distance of the points in the point cloud; and *class_threshold*, defining the distance from the simulated cloth to classify a point as ground or CFO. Three parameter combinations were explored (Table 1), and for each iteration, the segmentation of the ground and CFO's points was visually inspected as well as the % calculations of CFO points (Table S2).

(iii) Individual CFO detection, for which the LMF algorithm was applied (Popescu & Wynne, 2004), which required 3 attributes: *ws*, representing the diameter of the moving window used to detect the local height maxima; *shape*, defining the moving window shape, fixed as "circular" since it suited the best the morphotype of our CFOs; *hmin*, defining the height below which the point cannot be considered a local maxima. Three different values of *ws* were tried, and CFO detection was evaluated by

TABLE 1 Parameter combination values used for the sensitivity analysis of the three main processing steps of the proposed point cloud pipeline.

Noise detection	Ground classification	CFO top detection
sor (*k*, *m*)	csf (class threshold, cloth resolution)	lmf (ws, hmin)
(*m* = 3, *k* = 50)	(class threshold = 0.1) (cloth resolution = 0.05)	(ws = 0.3, hmin = 0.2)
(*m* = 3, *k* = 100)	(class threshold = 0.2) (cloth resolution = 0.05)	(ws = 0.4, hmin = 0.2)
(*m* = 5, *k* = 50)	(class threshold = 0.2) (cloth resolution = 0.10)	(ws = 0.5, hmin = 0.2)

the number of CFO identified by the *lmf* function and the % of deviation from the number of CFO manually detected in each study site.

2.7 | Evaluation metrics on CFOs detection and height estimation

The accuracy of the proposed approach was evaluated using different performance metrics. On the one hand, CFO detection accuracy was assessed by calculating Precision (*P*), Recall (*R*) and F_1-score (F_1):

$$P = \frac{TP}{TP + FP}; \quad R = \frac{TP}{TP + FN}; \quad F_1 = \frac{2 \times R \times P}{R + P}$$

where TP represents true positives, or CFO's tops that were detected, FP represents false positives or detected CFOs in the point cloud not corresponding to true CFOs, and FN represents false negatives, which refers to the number of CFOs that were not detected by the proposed method.

On the other hand, the quality of the height predictions was assessed with the coefficient of determination (R^2) and RMSE calculation (Chai & Draxler, 2014).

$$R^2 = 1 - \frac{\sum_{i=1}^{n} (y_i - \hat{y}_i)^2}{\sum_{i=1}^{n} (\bar{y}_i - y_i)^2}; \quad \text{RMSE} = \sqrt{\frac{1}{n} \sum_{i=1}^{n} (y_i - \hat{y}_i)^2}$$

where n represents the number of comparisons, y_i is the *true value* measured manually and $\hat{y}_i$ denotes the value predicted by the proposed pipeline. The R^2 and RMSE were calculated per each site with the free software R version 4.2.0 by using the functions *lm* and *rmse* of the *stats* and *Metrics* packages, respectively (Hamner & Frasco, 2018; R Core Team, 2024).

3 | RESULTS

3.1 | Photogrammetric analysis & manually extracted CFOs related metrics

A total of 7,295 images were collected for this study. An average of 1,459 ± 545 pictures was processed for the 3D analysis considering all five study sites, with a minimum of 771 pictures for Sheila Rock and a maximum of 2,142 pictures for Cala Portalò (Table S1). The five surveyed areas varied between 85 and 140 m^2, with an average of 107 ± 0.5 m^2, mapping a total of 535 m^2 of seabed. Using SfM-photogrammetry, dense point clouds with a 0.1 cm resolution were generated for each site, yielding an average of 117,793,135 ± 105,339,513 points per cloud. The 3D reconstructions exhibited an average RMSE of 0.18 ± 0.20 cm, which did not exceed 0.4 cm in any case. To optimize processing time, while maintaining accuracy, all point clouds were resampled to a 0.5 cm resolution for the analysis. This resampling produced average point counts of 7,222,607 ± 2,983,657 across all study sites. Regarding point clouds' density, all sites were inspected at 10 cm × 10 cm patch size obtaining average values ranging between 55,630 ± 54,288 points/dm^2 and 122,426 ± 159,445 points/dm^2 (Figure S1). Additional details such as number of images, total points count, RMSE and point densities at different classification stages (ground or CFO classified points) of each surveyed site are provided in Tables S1, S3 and Figure S1.

Manually inspecting the 3D digital reconstructions, each CFO was identified at the lowest taxonomic level possible. Overall, the dominant CFOs in all sites were gorgonian species, with an average density of 1.77 ± 0.99 (0.96–3.12) individuals/m^2 for *Paramuricea clavata* in Portofino and Punta Manara sites and 0.58 individuals/m^2 for *Eunicella singularis* in Cap de Creus (Table 2; Figure 4). The occasional occurrence of other CFOs was also recorded, in particular of the sponges *Sarcotragus foetidus* (4 individuals at Rampazzo

TABLE 2 Summary of abundances, densities, average heights (± standard deviation, SD) and height ranges per canopy-forming organism (CFO) and site obtained from the SfM-manual approach.

Site	CFO category	*n*	Density (n/m^2)	Average height (cm)	Height range (cm)
Punta del Faro	*Paramuricea clavata*	96	0.96	38.71 ± 12.08	20.40–79.00
	Dead *P. clavata*	1	0.01	54.10	–
Punta Vessinaro	*P. clavata*	152	1.09	45.46 ± 19.03	20.10–103.00
	Dead *P. clavata*	68	0.49	35.79 ± 14.94	20.20–84.30
Sheila Rock	*P. clavata*	191	1.91	49.00 ± 17.48	20.00–116.00
	Dead *P. clavata*	2	0.02	29.05 ± 0.49	28.70–29.40
	Savalia savaglia	29	0.29	46.82 ± 16.48	26.40–86.50
Rampazzo Point	*Axinella polypoides*	1	0.01	23.00	–
	Sarcotragus foetidus	4	0.05	26.82 ± 6.84	21.10–34.70
	P. clavata	265	3.12	47.17 ± 13.77	20.00–87.60
	Dead *P. clavata*	1	0.01	24.30	–
	S. savaglia	15	0.18	51.27 ± 16.85	32.50–93.60
Cala Portalò	*A. polypoides*	2	0.02	20.18 ± 0.88	18.70–21.80
	Eunicella singularis	64	0.58	23.43 ± 2.90	20.00–31.50

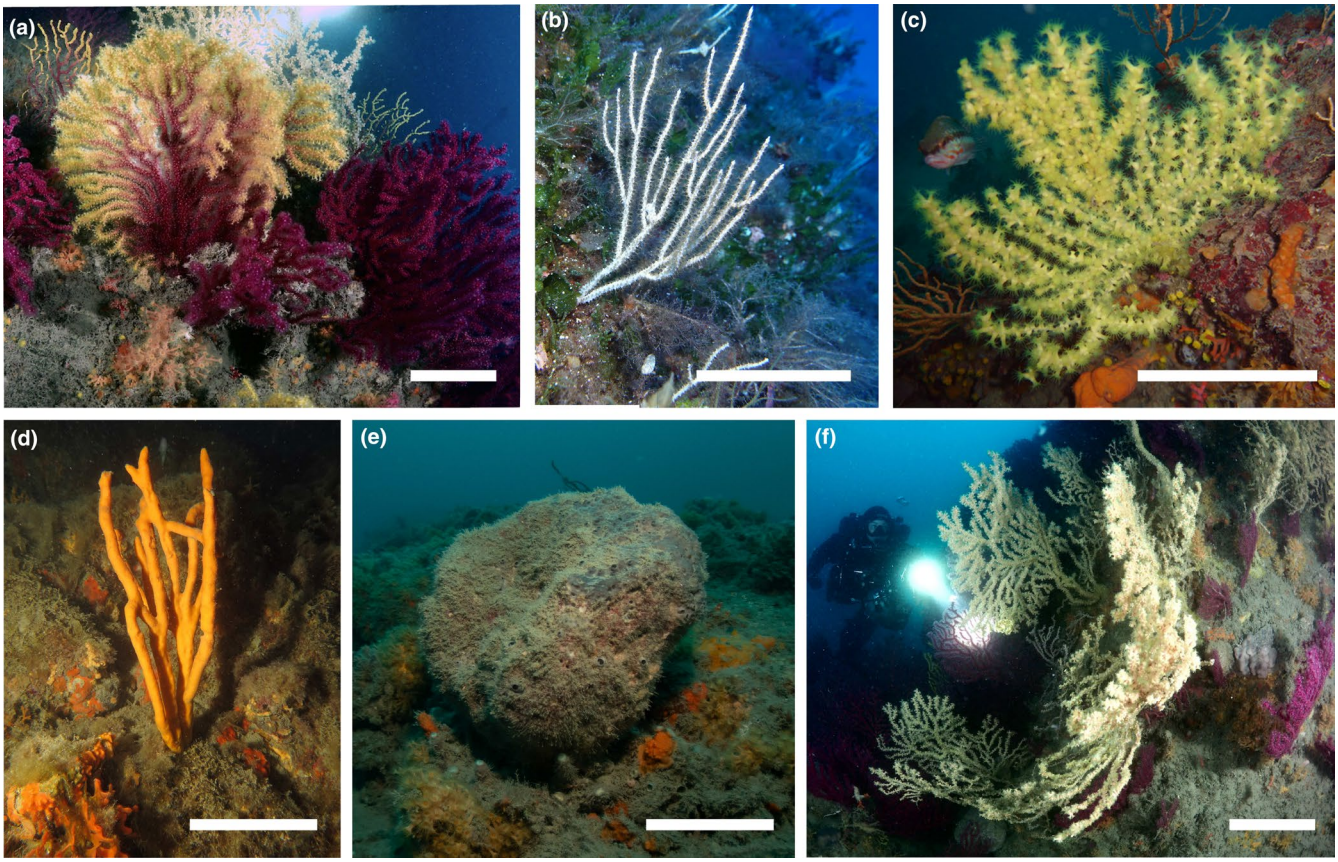

FIGURE 4 Image composite illustrating the vertically structuring organisms individualized during manual segmentation of the marine animal forests (MAFs) assessed during this study: (a) *Paramuricea clavata*, (b) *Eunicella singularis*, (c) *Savalia savaglia*; (d) *Axinella polypoides*; (e) *Sarcotragus foetidus*; (f) forests presenting both *P. clavata* and *S. savaglia*. Scale bars = 20 cm.

Point) and *Axinella polypoides* (1 and 2 individuals at Rampazzo Point and Cala Portalò, respectively), as well as of the zoanthid *Savalia savaglia* (0.18–0.29 individuals/m^2 at Rampazzo Point and Sheila Rock) (Table 2; Figure 4). Additionally, the manual inspection of the 3D reconstruction allowed the identification of dead CFOs, especially of the 68 dead gorgonians at Punta Vessinaro (Table 2). For more details regarding each typology of identified CFO (i.e., abundances, densities, average/maximum/minimum height), please see Table 2.

3.2 | Sensitivity analysis of the proposed pipeline

We performed a total of 27 pipeline iterations for each site (Table 1), resulting in 108 iterations (Table S2). With the sensitivity analysis, we selected a combination of parameters that maximized the agreement between manual and semi-automated results considering the following processing steps:

(i) For the noise detection, the SOR algorithm was implemented using 50 neighbouring points to calculate the mean average distance between points (*k*), and a multiplier (*m*) of 3 to establish the threshold for identifying noise. These values were selected because lower values of *k* or higher values of *m* resulted in many noise points being incorrectly classified, while higher values of *k* led to significantly longer processing times and often caused apical CFO ramifications to be classified as noise (Table S2).

(ii) For the ground classification, the CSF algorithm was applied with a particle distance of 0.05 m (*cloth_resolution*) between the simulated cloth particles, based on the average distance of points in the point cloud. This allowed to better adapt the cloth to the rugosity of the substrate. A *class_threshold* of 0.2 m was also set to prevent the misclassification of small terrain irregularities or small organisms. From this point onward, the minimum height for an organism to be considered as contributing to the canopy and, therefore, classified as a CFO by this approach is defined by this threshold value (Table S2).

(iii) For the individual CFO detection, the LMF algorithm (Popescu & Wynne, 2004) was applied with a diameter of 0.35 m (*ws*), which represents the diameter of the moving window used to detect the CFO tops. A minimum height of 0.2 m (*hmin*) was also established, below which the point will not be considered as a part of a CFO, in accordance with the previously defined threshold. The window size was chosen as a compromise: using smaller *ws* values often led to the algorithm overestimating the number of detected CFO by counting wider organisms as multiple CFO,

while larger values of *ws* caused close organisms to be clustered together and classified as a single CFO (Table S2).

3.3 | Semantic segmentation results and comparison with manually extracted metrics

Considering all sites, average CFO's density values of 1.72 ± 1.10 CFOs/m^2 and 1.96 ± 0.63 CFOs/m^2 were obtained with the manual and semi-automated methods, respectively. The highest densities and average CFOs heights were recorded in Rampazzo Point (3.35 CFOs/m^2; 47.17 ± 13.77 cm) and Sheila Rock (2.20 CFOs/m^2; 49.00 ± 17.48 cm) with the manual approach. Conversely, with the proposed pipeline, the highest densities were recorded in Rampazzo Point (2.73 CFOs/m^2) and Punta Vessinaro (2 CFOs/m^2), while the highest height averages were found in Sheila Rock (65.36 ± 27.57 cm) and Rampazzo Point (61.03 ± 24.67 cm) (Table 3).

To assess the accuracy of the proposed point cloud processing pipeline, a pool of quantitative metrics was applied to evaluate CFOs detection and height estimation. For point cloud segmentation and CFOs detection, precision, recall and F_1-score were calculated. The pipeline performed well in detecting CFOs across 4 out of 5 sites (F_1-scores ranging from 0.79 to 0.85), while Cala Portalò clearly represented an outlier (F_1-score = 0.55) (Table 4; Figures 5 and 6).

To assess the ability of the proposed approach to estimate CFOs heights, results of the semi-automated pipeline and the manually obtained heights were compared, linear regression analysis was carried out, and R^2 coefficient and RMSE were calculated. An average R^2 of 0.55 ± 0.29 was obtained, with Punta Vessinaro and Punta del Faro holding the highest coefficient values (0.81 and 0.68, respectively), while Cala Portalò presented the lowest R^2 (0.06). In terms of RMSE value, an average of 17.97 ± 6.93 cm was obtained, with the lowest values calculated for Punta del Faro (10.43 cm) and Punta Vessinaro (10.53 cm), and the highest present in Sheila Rock (24.64 cm) (Table 4; Figure 7). The heights derived from the proposed approach showed a general overestimation of CFOs heights, especially evident for those sites with lower R^2 and higher RMSE (Sheila Rock, Rampazzo Point and Cala Portalò) (Figure 7c–e), being also the ones presenting highly irregular substrates (e.g. frequent changes in slope inclination; Figures 5c and 6).

3.4 | MAF canopy estimation

In addition to the CFOs detection and height estimation, the pipeline allowed to estimate also the overall canopy volume provided by the MAF at each study site, as well as the canopy occupancy by means of the voxelization of the segmented point clouds (Figure 8). An average canopy volume of 5.95 ± 3.84 m^3 and canopy occupancy of (60 ± 48) × 10^{-3} m^3/m^2 were provided among all study sites. Overall, apart from Cala Portalò, the sites presenting the greater CFO

TABLE 3 Summary of abundances, densities, average heights (± standard deviation, SD), height ranges, canopy volumes, canopy occupancy and time invested in the analysis per method and site.

Site	Method	Time (h)	*n*	Density (n/m^2)	Average height (cm)	Height range (cm)	Canopy volume (m^3)	Canopy occupancy (m^3/m^2)
Punta del Faro	Manual	1:15	97	0.97	38.71 ± 12.08	20.40–79.0	–	–
	Semi-automatic	0:09	119	1.19	45.52 ± 16.10	20.35–88.17	2.14	21.14×10^{-3}
Punta Vessinaro	Manual	3:40	210	1.5	45.46 ± 19.03	20.1–103.0	–	–
	Semi-automatic	0:11	281	2	51.02 ± 23.25	20.33–142.80	5.58	39.88×10^{-3}
Sheila Rock	Manual	4:20	220	2.2	49.00 ± 17.48	20.00–116.00	–	–
	Semi-automatic	0:12	186	1.92	65.36 ± 27.57	20.06–155.81	7.35	73.5×10^{-3}
Rampazzo Point	Manual	5:15	285	3.35	47.17 ± 13.77	20.00–87.6	–	–
	Semi-automatic	0:13	232	2.73	61.03 ± 24.67	20.02–135.6	11.72	137.82×10^{-3}
Cala Portalò	Manual	4:30	64	0.58	23.43 ± 2.90	20.00–31.50	–	–
	Semi-automatic	0:11	146	1.33	41.74 ± 19.54	20.22–96.04	2.95	26.78×10^{-3}

TABLE 4 Summary of metrics calculated to quantitatively evaluate canopy forming organisms (CFOs) detection and height estimation.

	CFO detection						CFO height estimation	
Site	True positives	False positives	False negatives	Precision (*P*)	Recall (*R*)	F_1-score	R^2	RMSE (cm)
Punta del Faro	89	25	11	0.78	0.89	0.83	0.68	10.43
Punta Vessinaro	202	62	8	0.77	0.96	0.85	0.81	10.53
Sheila Rock	161	25	59	0.87	0.73	0.79	0.56	24.64
Rampazzo Point	205	16	80	0.93	0.72	0.81	0.62	22.75
Cala Portalò	92	48	101	0.66	0.48	0.55	0.06	21.52

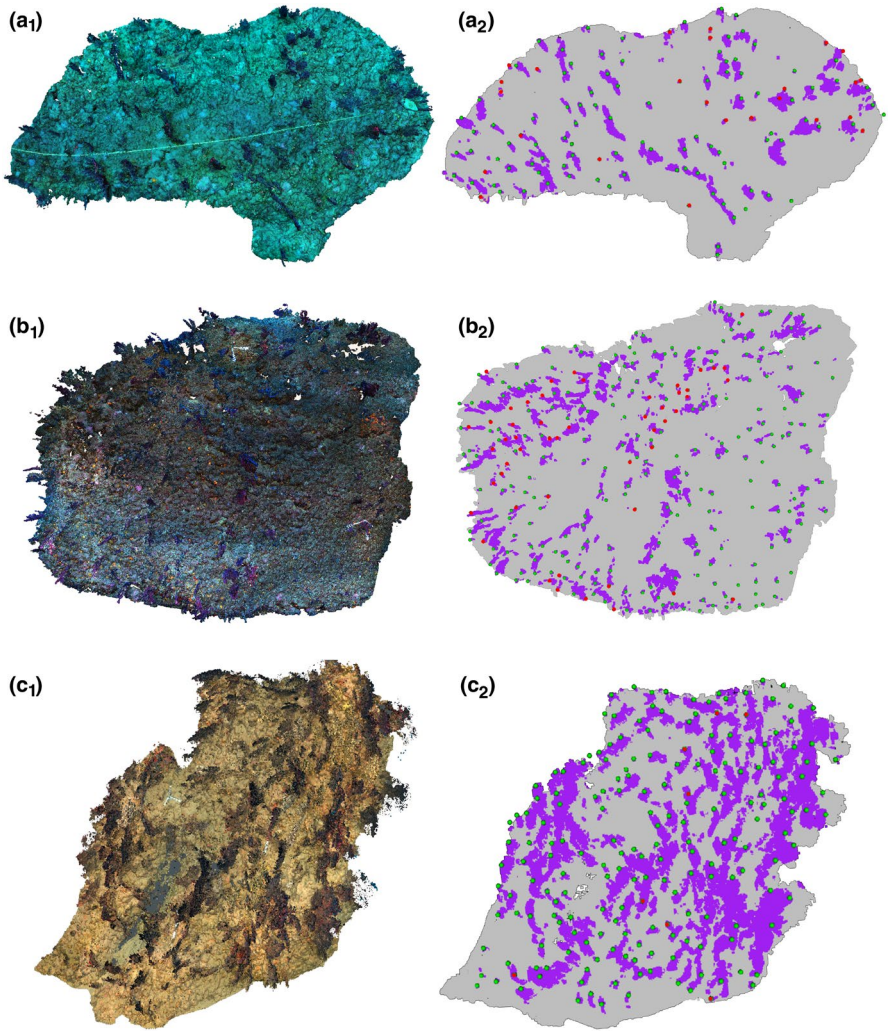

FIGURE 5 Image composite illustrating the 3D reconstructions of Punta del Faro (a), Punta Vessinaro (b) and Sheila Rock (c), along with the results after the ground classification and single canopy forming organism (CFO) detection steps during the point cloud processing. Please note all figures subscripted "1" represent the RGB coloured point clouds, while all subscripted "2" represent the binary segmented point clouds where ground points are represented in grey and CFO's points in purple. Green bullet points depict the true positive detections of CFOs tops, while red bullet points depict the false-positive detections.

densities and average heights displayed the highest canopy volumes and occupancies, represented by Rampazzo Point (11.72 m^3 and 137.82×10^{-3} m^3/m^2) and Sheila Rock (7.35 m^3 and 73.5×10^{-3} m^3/m^2) (Tables 2 and 3; Figure 8).

4 | DISCUSSION

As terrestrial forests, MAFs are characterized by a complex 3D framework, a feature often neglected or not fully assessed in monitoring programs due to the lack of cost-effective methods to properly approach it (Orejas et al., 2022; Rossi et al., 2021). In this context, we advocate for leveraging the theoretical and methodological knowledge from terrestrial forestry when assessing vegetation canopies and encourage its application to the marine environment. Even though the direct transfer of land-based approaches can be challenging due to the change of medium and habitat (Pulido Mantas, Roveta, Calcinai, di Camillo, et al., 2023), testing pipelines commonly used in forest inventories to 3D data derived from optical and/or acoustic sources in marine studies represents a promising

research direction. Therefore, with this study we aim establishing a novel framework by proposing the application of standard forestry segmentation procedures for the classification and characterization of marine habitat formers (Figure 3), a path that remained untrodden until now.

The results obtained from the application of the *lidR* R package (Roussel et al., 2020) to process and analyse SfM-derived point clouds demonstrated the huge potential of this method for the creation of MAF inventories. In fact, the proposed semi-automated approach achieved a good detection accuracy comparable with tree detection ones (Saeed et al., 2024; Zhang et al., 2025), obtaining, except for Cala Portalò, high precision, recall and F_1-score values (over 0.76, 0.71 and 0.79, respectively) (Table 4; Figures 5 and 6). Considering the recorded misclassifications, they generally resulted from the use of a fixed circular search-window of 0.35 m ø, causing: (i) the undersegmentation of CFOs by clustering nearby organisms when closely located; or (ii) the oversegmentation of CFOs by double-counting very wide single organisms (Figures 5 and 6).

While CFOs detection was generally successful, the accuracy of height estimation was limited, with R^2 values ranging between 0.06 and 0.81, and an average RMSE of 17.97 ± 6.93 cm (Table 4; Figure 7). The higher RMSE values coincided with the lower R^2 coefficients in those sites characterized by highly irregular substrates and frequent slope changes (namely, Sheila Rock, Rampazzo Point and Cala Portaló) (Table 4). In fact, after inspecting the spatial distribution of the CFOs contributing the most to the overall error (represented as outliers in Figure 7 scatterplots), it was clear how the proposed pipeline highly overestimated the height of CFOs growing on steep slope changes (e.g., rock outcrops, walls, crevices), while it could not detect organisms with height values close to the estimation error (i.e., RMSE; Table 4). The strong influence of topography on tree detection and height assessment in terrestrial forests is well documented (Graham et al., 2019; Khosravipour et al., 2015; Q. Li et al., 2025; Meng et al., 2010; Mielcarek et al., 2018); however, in the case of MAFs, beside the effects of terrain slope and orientation on point cloud ground classification and height normalization, an additional confounding factor is in play. CFOs, here represented by sessile filter- and suspension-feeders, typically do not exhibit plant-like tropisms (e.g., gravitropism, phototropism), resulting in irregular growth orientations and non-spatially homogeneous growth patterns in the

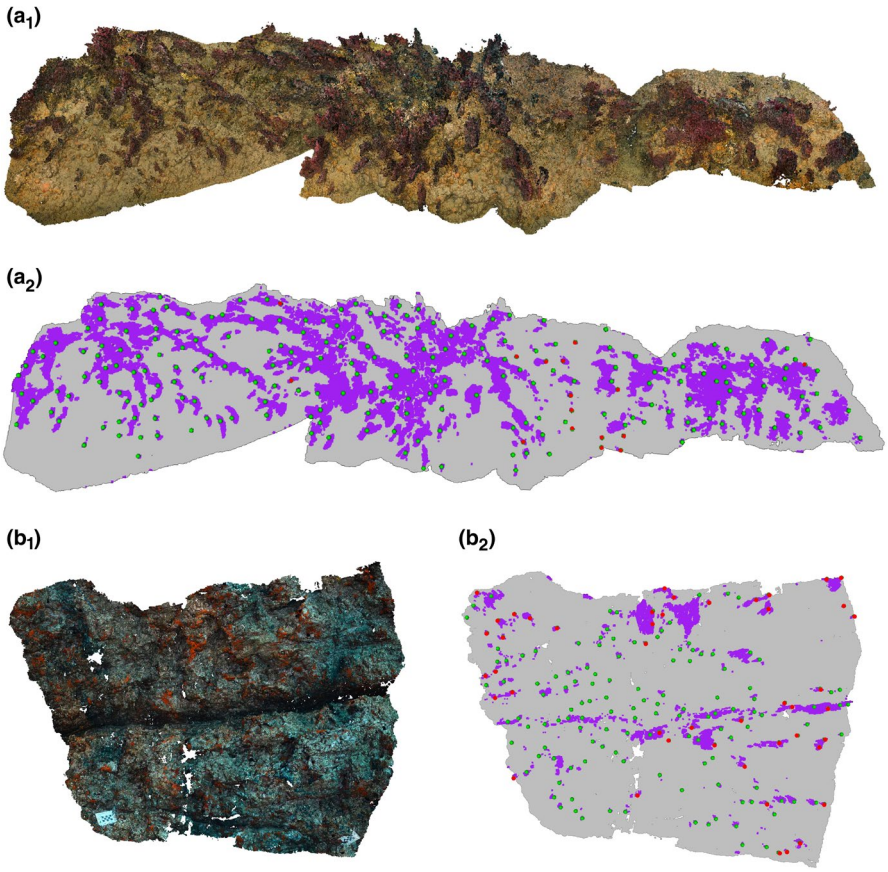

FIGURE 6 Image composite illustrating the 3D reconstructions of Rampazzo Point (a) and Cala Portalò (b), along with the results after the ground classification and single canopy forming organism (CFO) detection steps during the point cloud processing. Please note all figures subscripted "1" represent the RGB coloured point clouds, while all subscripted "2" represent the binary segmented point clouds where ground points are represented in grey and CFO's points in purple. Green bullet points depict the true positive detections of CFOs tops, while red bullet points depict the false-positive detections.

FIGURE 7 Comparison of manually measured canopy forming organisms (CFOs) height and height calculated by the proposed approach for each site. On the left, the linear regressions (blue lines) with 95% confidence intervals (greyish area), and 1:1 relationship (dashed red lines); on the right, frequency plots of the high values comparison depicting manually extracted measurements (yellow bars) and height calculated by the proposed approach (purple bars).

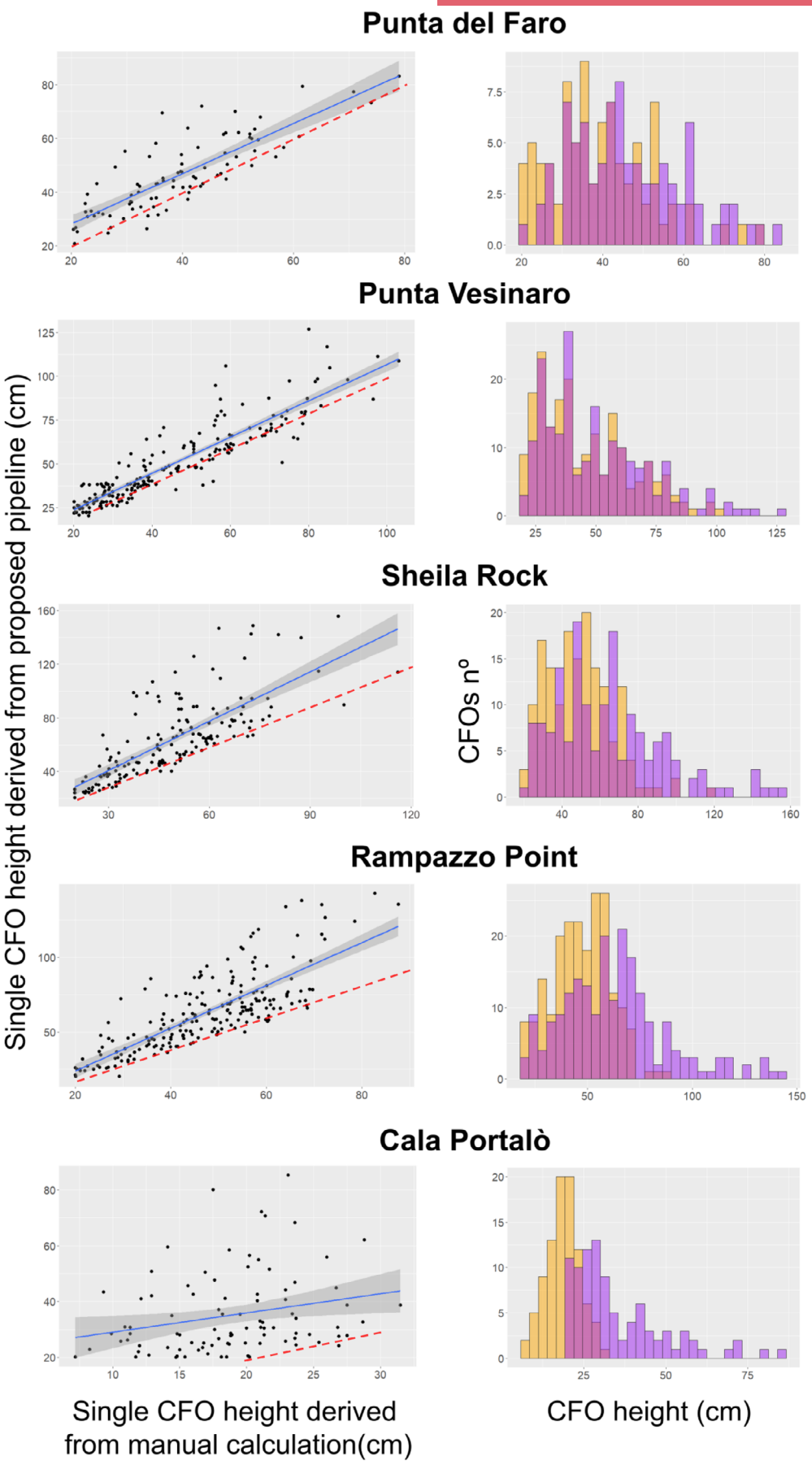
Punta del Faro
Punta Vesinaro
Sheila Rock
Rampazzo Point
Cala Portalò
Single CFO height derived from proposed pipeline (cm)
CFOs n°
Single CFO height derived from manual calculation(cm)
CFO height (cm)

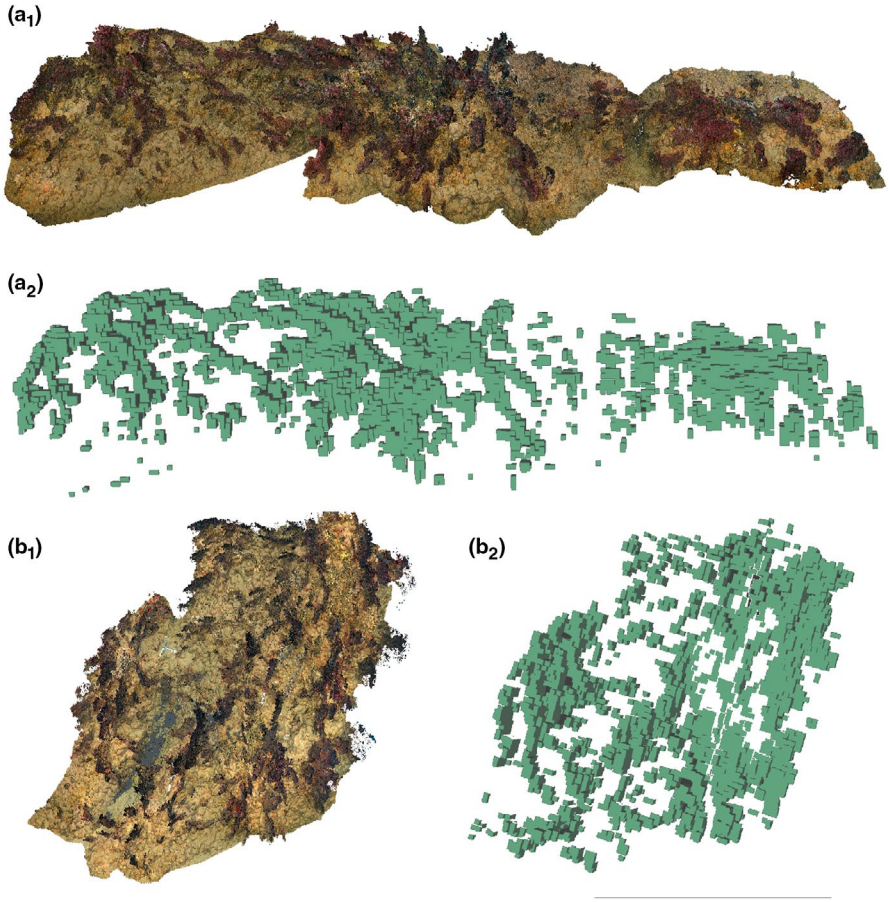

FIGURE 8 Examples of the results after the voxelization (0.1 m × 0.1 m × 0.1 m voxel size) of the point clouds classified as canopy forming organisms (CFOs) at Rampazzo Point (a) and Sheila Rock (b), the two sites displaying the highest canopy values. Please note all subscripted "1" subfigures represent the RGB coloured point clouds, while all subscripted "2" represent the voxelized "canopy espace" of the assessed marine animal forests.

search for current exposure (Rees, 1972; Riedl & Forstner, 1968). The synergy of all previously mentioned factors introduces substantial uncertainty in CFOs height estimation between the proposed automated pipeline and manual measurements. More specifically, the displacement of the detected highest point of the CFOs after normalization, or the misidentification of the substrate immediately beneath the detected CFOs top as the base (mainly on vertical or steeply inclined surfaces), resulted in a systematic overestimation of heights.

In this study, Cala Portalò represents the perfect example of the conditions under which the pipeline fails to characterize a MAF (Figures 6b and 7). The low vertical development and unique candelabra-like morphotype (Gori et al., 2012) of the dominant CFO of the site (*Eunicella singularis*) and the highly irregular topography (Figure 6b) resulted in poor classification results, often identifying substrate irregularities as CFOs and largely overestimating CFOs heights, ultimately ending up in an overall inaccurate CFOs detection and height estimation (Table 4). Apart from this specific case, the proposed pipeline showed promising results when applied to the other sites here considered. However, being *Paramuricea clavata* the other dominant CFO, further research should include MAFs formed by CFOs representing other species or morphotypes, thus allowing for more general conclusions in the search for a one-size-fits-all tool to assess canopy-forming MAFs.

Although canopy occlusion was not identified as one of the main limitations in this study, the application of optical-based methods to tightly packed MAFs could still present methodological constraints. Such occlusion may lead to data voids that hinder accurate ground detection and subsequent height estimations (Cao et al., 2023; Gassilloud et al., 2025). To minimize this issue, it is essential to consider point cloud density through the workflow, ensuring a minimum density across the various point cloud levels (Figure S1) (LaRue et al., 2022). Adapting sampling strategies to MAFs features (e.g., distance to the substrate, increasing sampling effort, use of different lenses) could further reduce occlusion effects. Among the emerging approaches to mitigate the issue in terrestrial studies, there are the fusion of multi-source data through the integration of techniques such as LiDAR and multispectral imagery (Chen et al., 2017), and the use of deep learning algorithms (Bornand et al., 2024). Considering the rapid advancements in underwater LiDAR-detection systems (Collings et al., 2020; Filisetti et al., 2018; Lin et al., 2023), coupling SfM with LiDAR could represent a promising alternative, potentially ensuring a greater penetration through the MAFs canopy and the generation of denser point clouds (Puliti et al., 2020).

In recent years, 3D point cloud representation and classification have become major research hotspots in computer vision, with applications across diverse fields such as robotics, virtual reality and autonomous driving (Fernandes et al., 2021; Hackel et al., 2017; Li et al., 2024; Zhang et al., 2023). Each year, new algorithms and hybrid techniques are developed to classify and extract information from 3D forestry data, often combining photogrammetry, LiDAR,

multispectral imagery and/or artificial intelligence (Burmeister et al., 2025; Carbonell-Rivera et al., 2024; Coops et al., 2021; Kuang et al., 2024; Liu et al., 2024; Ma et al., 2023; Wu et al., 2025). Following examples in the literature that promote the exchange of concepts, methods and technologies between marine and terrestrial ecologists (D'Urban Jackson et al., 2020; Munguia & Ojanguren, 2015; Torres-Pulliza et al., 2020; Webb, 2012), our proposed pipeline aims to establish a common framework for the assessment of marine and terrestrial forests. This framework is intended to facilitate the transfer and testing of emerging approaches to overcome the current methodological challenges identified in this study, and to define a set of suitable CFOs for which this methodology could support the implementation of medium to large-scale systematic monitoring programs.

For a long time, MAFs assessment has relied on manual *in situ* two-dimensional measurements (i.e., CFO's height, width and/or density), which are time consuming, expensive and limited in spatio-temporal scales (i.e., Figuerola-Ferrando et al., 2024; Jacobsen et al., 2024; Ponti et al., 2018; Zentner et al., 2023). However, canopy-forming MAFs represent a dynamic 3D interface between CFOs and the water column, influencing local physico-chemical parameters, generating ecological gradients within the canopy (Guizien & Ghisalberti, 2017) and supporting a wide range of ecosystem services (Gómez-Gras et al., 2021). Even if the ecological importance of the canopy is widely recognized, most studies have addressed this feature qualitatively or indirectly, with only a few examples adopting a truly 3D perspective (Cerpovicz & Lasker, 2021; Palma et al., 2018; Smith et al., 2022). Although not without limitations, the proposed pipeline enables, for the first time, a standardized semi-automatic 3D quantification of the MAF canopy volume, a key metric that expands the suite of tools available to characterize soft-bodied CFOs, organisms historically overlooked due to the lack of suitable techniques (Rossi et al., 2021; Smith et al., 2022). By estimating the canopy volume, it becomes possible to evaluate the actual space that MAFs offer to the associated communities, which can serve as a proxy for habitat capacity and integrity (Rossi et al., 2017). This opens new opportunities to investigate these habitats from a multidisciplinary perspective, integrating hydrodynamic, physical and biogeochemical approaches. Consequently, the ability to numerically quantify this feature represents a significant step forward in the monitoring and management of these habitats, promoting a shift from species- or population-level analyses towards a community-level understanding.

To conclude, this study represents a pioneering step in applying 3D optical-based mapping combined with a semi-automatic point cloud classification pipeline to enable scalable surveys of vulnerable marine ecosystems. While certain limitations remain, the proposed approach offers a cost-effective and innovative framework for the assessment of MAFs, providing new opportunities to characterize soft-bodied CFOs as well as MAFs canopy volumes and occupancies. Furthermore, integrating this framework with unmanned or remotely operated underwater vehicles and AI could unlock its full potential, optimizing large-scale applications and classification workflows (Alexandris et al., 2024; Marlow et al., 2024; Remmers et al., 2024). In this context, the proposed approach constitutes an essential contribution towards the sustainable management of marine ecosystems, as established by the Marine Strategy Framework Directive, while supporting the Sustainable Development Goal 14 and the global objectives outlined in the UN 2030 Agenda.

AUTHOR CONTRIBUTIONS

Conceptualization: Carlo Cerrano and Torcuato Pulido Mantas; Data curation: Torcuato Pulido Mantas and Camilla Roveta; formal analysis: Manuja Promodya Hendawitharana, Torcuato Pulido Mantas and Camilla Roveta; funding acquisition: Carlo Cerrano, Joaquim Garrabou, Torcuato Pulido Mantas and Camilla Roveta; methodology: Torcuato Pulido Mantas; resources: Joaquim Garrabou, Nils Lucas Jacobsen, Marco Palma, Ubaldo Pantaleo and Torcuato Pulido Mantas; visualization: Martina Coppari, Cristina Gioia Di Camillo, Torcuato Pulido Mantas and Camilla Roveta; roles/writing—original draft: Torcuato Pulido Mantas and Camilla Roveta; writing—review and editing: Carlo Cerrano, Martina Coppari, Cristina Gioia Di Camillo, Joaquim Garrabou, Manuja Promodya Hendawitharana, Nils Lucas Jacobsen, Marco Palma and Ubaldo Pantaleo.

ACKNOWLEDGEMENTS

Authors are grateful to Reef Alert Network, especially to all volunteers taking part in the activities (Bruno Borelli, Romano Rampazzo, Sheila Rinaldi, Martin Demper and Arno van Dort) and to Portofino Divers for the logistic support. Authors would also like to thank Tritonia Scientific Ltd. for the logistic and scientific support in the context of the Assemble Plus Project "Temperate Biogenic Reefs 3D-BioNET". Authors are thankful to Bruno Borelli, who provided some photographs needed to create Figures 2 and 4. Finally, authors would also like to thank the Editor and the Reviewers for their work and precious comments, which undoubtedly help to improve the manuscript.

FUNDING INFORMATION

The current work was developed under the National Recovery and Resilience Plan (NRRP), Mission 4, Component 2, Investment 1.4—Call for tender No. 3138 of 16 December 2021 rectified by Decree n.3175 of 18 December 2021 of the Italian Ministry of University and Research funded by the European Union—NextGenerationEU; Award Number: Project code CN_00000033, Concession Decree No. 1034 of 17 June 2022 adopted by the Italian Ministry of University and Research, CUP D33C22000960007 and D31B21008270007, Project title "National Biodiversity Future Center—NBFC". This work also received part of the financial support from: the European Union's Horizon 2020 research and innovation programme, ASSEMBLE Plus Project (grant number 12091); the Interreg Med MPA Engage "Engaging Mediterranean key actors in Ecosystem Approach to manage Marine Protected Areas to face Climate change" (grant number 5216); and "Progetto di valorizzazione del patrimonio naturale sommerso di Punta Manara. Ricostruzione 3D delle foreste di gorgonie." funded by Mercuria Energy Group Ltd.

CONFLICT OF INTEREST STATEMENT

The authors declare that they have no known competing financial interests or personal relationships that could have appeared to influence the work reported in this paper.

PEER REVIEW

The peer review history for this article is available at https://www.webofscience.com/api/gateway/wos/peer-review/10.1111/2041-210x.70242.

DATA AVAILABILITY STATEMENT

The 3D point clouds (at 0.5 and 1 cm resolutions) and the R code used to implement the proposed approach are available at the following link: https://doi.org/10.5281/zenodo.18155450 (Pulido Mantas et al., 2026).

ORCID

Torcuato Pulido Mantas https://orcid.org/0000-0002-0260-8373
Camilla Roveta https://orcid.org/0000-0001-8629-7113
Manuja Promodya Hendawitharana https://orcid.org/0000-0002-6272-1730

REFERENCES

Alexandris, C., Papageorgas, P., & Piromalis, D. (2024). Positioning systems for unmanned underwater vehicles: A comprehensive review. *Applied Sciences*, *14*(21), 21. https://doi.org/10.3390/app14219671

Bayley, D. T. I., & Mogg, A. O. M. (2020). A protocol for the large-scale analysis of reefs using structure from motion photogrammetry. *Methods in Ecology and Evolution*, *11*(11), 1410–1420. https://doi.org/10.1111/2041-210X.13476

Borghi, C., Francini, S., D'Amico, G., Valbuena, R., Chirici, G., Borghi, C., Francini, S., D'Amico, G., Valbuena, R., & Chirici, G. (2025). Advancements in Forest monitoring: Applications and perspectives of airborne laser scanning and complementarity with satellite optical data. *Land*, *14*(3), 567. https://doi.org/10.3390/land14030567

Bornand, A., Abegg, M., Morsdorf, F., & Rehush, N. (2024). Completing 3D point clouds of individual trees using deep learning. *Methods in Ecology and Evolution*, *15*(11), 2010–2023. https://doi.org/10.1111/2041-210X.14412

Bosch, N. E., Espino, F., Tuya, F., Haroun, R., Bramanti, L., & Otero-Ferrer, F. (2023). Black coral forests enhance taxonomic and functional distinctiveness of mesophotic fishes in an oceanic Island: Implications for biodiversity conservation. *Scientific Reports*, *13*(1), 4963. https://doi.org/10.1038/s41598-023-32138-x

Burmeister, J.-M., Tockner, A., Reder, S., Engel, M., Richter, R., Mund, J.-P., & Döllner, J. (2025). *treeX: Unsupervised tree instance segmentation in dense Forest point clouds*. (No. arXiv:2509.03633). arXiv https://doi.org/10.48550/arXiv.2509.03633

Burns, J. H. R., Delparte, D., Gates, R. D., & Takabayashi, M. (2015). Integrating structure-from-motion photogrammetry with geospatial software as a novel technique for quantifying 3D ecological characteristics of coral reefs. *PeerJ*, *3*, e1077. https://doi.org/10.7717/peerj.1077

Cao, Y., Ball, J. G. C., Coomes, D. A., Steinmeier, L., Knapp, N., Wilkes, P., Disney, M., Calders, K., Burt, A., Lin, Y., & Jackson, T. D. (2023). Benchmarking airborne laser scanning tree segmentation algorithms in broadleaf forests shows high accuracy only for canopy trees. *International Journal of Applied Earth Observation and Geoinformation*, *123*, 103490. https://doi.org/10.1016/j.jag.2023.103490

Carbonell-Rivera, J. P., Estornell, J., Ruiz, L. Á., Crespo-Peremarch, P., Almonacid-Caballer, J., & Torralba, J. (2024). Class3Dp: A supervised classifier of vegetation species from point clouds. *Environmental Modelling & Software*, *171*, 105859. https://doi.org/10.1016/j.envsoft.2023.105859

Carpine, C., & Grasshoff, M. (1975). Les gorgonaires de la Méditerranée. *Bulletin de l'Institut Océanographique de Monaco*, *17*, 1–140.

Cerpovicz, A. F., & Lasker, H. R. (2021). Canopy effects of octocoral communities on sedimentation: Modern baffles on the shallow-water reefs of St. John, USVI. *Coral Reefs*, *40*(2), 295–303. https://doi.org/10.1007/s00338-021-02053-6

Cerrano, C., Bastari, A., Calcinai, B., Di Camillo, C., Pica, D., Puce, S., Valisano, L., & Torsani, F. (2019). Temperate mesophotic ecosystems: Gaps and perspectives of an emerging conservation challenge for the Mediterranean Sea. *The European Zoological Journal*, *86*(1), 370–388. https://doi.org/10.1080/24750263.2019.1677790

Cerrano, C., Danovaro, R., Gambi, C., Pusceddu, A., Riva, A., & Schiaparelli, S. (2010). Gold coral (*Savalia savaglia*) and gorgonian forests enhance benthic biodiversity and ecosystem functioning in the mesophotic zone. *Biodiversity and Conservation*, *19*(1), 153–167. https://doi.org/10.1007/s10531-009-9712-5

Chai, T., & Draxler, R. R. (2014). Root mean square error (RMSE) or mean absolute error (MAE)?—Arguments against avoiding RMSE in the literature. *Geoscientific Model Development*, *7*(3), 1247–1250. https://doi.org/10.5194/gmd-7-1247-2014

Chen, Z., Gao, B., Devereux, B., Chen, Z., Gao, B., & Devereux, B. (2017). State-of-the-art: DTM generation using airborne LIDAR data. *Sensors*, *17*(1), 150. https://doi.org/10.3390/s17010150

Collings, S., Martin, T. J., Hernandez, E., Edwards, S., Filisetti, A., Catt, G., Marouchos, A., Boyd, M., & Embry, C. (2020). Findings from a combined subsea LiDAR and multibeam survey at Kingston reef, Western Australia. *Remote Sensing*, *12*(15), 15. https://doi.org/10.3390/rs12152443

Coops, N. C., Tompalski, P., Goodbody, T. R. H., Queinnec, M., Luther, J. E., Bolton, D. K., White, J. C., Wulder, M. A., van Lier, O. R., & Hermosilla, T. (2021). Modelling lidar-derived estimates of forest attributes over space and time: A review of approaches and future trends. *Remote Sensing of Environment*, *260*, 112477. https://doi.org/10.1016/j.rse.2021.112477

de Oliveira, L. M. C., Lim, A., Conti, L. A., & Wheeler, A. J. (2022). High-resolution 3D mapping of cold-water coral reefs using machine learning. *Frontiers in Environmental Science*, *10*, 1044706. https://doi.org/10.3389/fenvs.2022.1044706

D'Urban Jackson, T., Williams, G. J., Walker-Springett, G., & Davies, A. J. (2020). Three-dimensional digital mapping of ecosystems: A new era in spatial ecology. *Proceedings of the Royal Society B: Biological Sciences*, *287*(1920), 20192383. https://doi.org/10.1098/rspb.2019.2383

FAO. (1948). Forest resources of the world. *Unasylva*, *2*(4), 161–182.

Fassnacht, F. E., White, J. C., Wulder, M. A., & Næsset, E. (2024). Remote sensing in forestry: Current challenges, considerations and directions. *Forestry: An International Journal of Forest Research*, *97*(1), 11–37. https://doi.org/10.1093/forestry/cpad024

Fernandes, D., Silva, A., Névoa, R., Simões, C., Gonzalez, D., Guevara, M., Novais, P., Monteiro, J., & Melo-Pinto, P. (2021). Point-cloud based 3D object detection and classification methods for self-driving applications: A survey and taxonomy. *Information Fusion*, *68*, 161–191. https://doi.org/10.1016/j.inffus.2020.11.002

Ferretti, M. (2013). Chapter 1—Forest monitoring: An introduction. In M. Ferretti & R. Fischer (Eds.), *Developments in environmental science* (Vol. *12*, pp. 3–18). Elsevier. https://doi.org/10.1016/B978-0-08-098222-9.00001-7

Figuerola-Ferrando, L., Garrabou, J., & Linares, C. (2024). A rapid assessment method to monitor the health status of habitat-forming species in coastal benthic ecosystems. *Aquatic Conservation: Marine*

and Freshwater Ecosystems, *34*(3), e4120. https://doi.org/10.1002/aqc.4120

Filisetti, A., Marouchos, A., Martini, A., Martin, T., & Collings, S. (2018). *Developments and applications of underwater LiDAR systems in support of marine science*. Oceans 2018 MTS/IEEE Charleston, 1–10 https://doi.org/10.1109/OCEANS.2018.8604547

Gambrel, B., & Lasker, H. R. (2016). Interactions in the canopy among Caribbean reef octocorals. *Marine Ecology Progress Series*, *546*, 85–95. https://doi.org/10.3354/meps11670

Garrabou, J., Bensoussan, N., Di Franco, A., Boada, J., Cebrian, E., Santamaría, J., Guala, I., Grech, D., Cerrano, C., Pulido Mantas, T., Jou, M., Marambio, M., & Azzurro, E. (2022). *Monitoring climate-related responses in mediterranean marine protected areas and beyond: Eleven standard protocols*. https://doi.org/10.13039/501100011033

Garrabou, J., Gómez-Gras, D., Medrano, A., Cerrano, C., Ponti, M., Schlegel, R., Bensoussan, N., Turicchia, E., Sini, M., Gerovasileiou, V., Teixido, N., Mirasole, A., Tamburello, L., Cebrian, E., Rilov, G., Ledoux, J.-B., Souissi, J. B., Khamassi, F., Ghanem, R., & Harmelin, J.-G. (2022). Marine heatwaves drive recurrent mass mortalities in the Mediterranean Sea. *Global Change Biology*, *28*(19), 5708–5725. https://doi.org/10.1111/gcb.16301

Gassilloud, M., Koch, B., & Göritz, A. (2025). Occlusion mapping reveals the impact of flight and sensing parameters on vertical forest structure exploration with cost-effective UAV based laser scanning. *International Journal of Applied Earth Observation and Geoinformation*, *139*, 104493. https://doi.org/10.1016/j.jag.2025.104493

Gómez-Gras, D., Linares, C., Dornelas, M., Madin, J. S., Brambilla, V., Ledoux, J.-B., López-Sendino, P., Bensoussan, N., & Garrabou, J. (2021). Climate change transforms the functional identity of Mediterranean coralligenous assemblages. *Ecology Letters*, *24*(5), 1038–1051. https://doi.org/10.1111/ele.13718

González-Rivero, M., Harborne, A. R., Herrera-Reveles, A., Bozec, Y.-M., Rogers, A., Friedman, A., Ganase, A., & Hoegh-Guldberg, O. (2017). Linking fishes to multiple metrics of coral reef structural complexity using three-dimensional technology. *Scientific Reports*, *7*(1), 13965. https://doi.org/10.1038/s41598-017-14272-5

Gori, A., Bavestrello, G., Grinyó, J., Dominguez-Carrió, C., Ambroso, S., & Bo, M. (2017). Animal forests in deep coastal bottoms and continental shelf of the Mediterranean Sea. In S. Rossi, L. Bramanti, A. Gori, & C. Orejas (Eds.), *Marine animal forests. The ecology of benthic biodiversity hotspots* (pp. 1–27). Springer International Publishing. https://doi.org/10.1007/978-3-319-17001-5_5-1

Gori, A., Bramanti, L., López-González, P., Thoma, J. N., Gili, J.-M., Grinyó, J., Uceira, V., & Rossi, S. (2012). Characterization of the zooxanthellate and azooxanthellate morphotypes of the Mediterranean gorgonian *Eunicella singularis*. *Marine Biology*, *159*(7), 1485–1496. https://doi.org/10.1007/s00227-012-1928-3

Graham, A., Coops, N. C., Wilcox, M., Plowright, A., Graham, A., Coops, N. C., Wilcox, M., & Plowright, A. (2019). Evaluation of ground surface models derived from unmanned aerial systems with digital aerial photogrammetry in a disturbed conifer forest. *Remote Sensing*, *11*(1), 84. https://doi.org/10.3390/rs11010084

Guizien, K., & Ghisalberti, M. (2017). Living in the canopy of the animal Forest: Physical and biogeochemical aspects. In S. Rossi, L. Bramanti, A. Gori, & C. Orejas (Eds.), *Marine animal forests. The ecology of benthic biodiversity hotspots* (pp. 1–22). Springer International Publishing. https://doi.org/10.1007/978-3-319-17001-5_14-1

Hackel, T., Savinov, N., Ladicky, L., Wagner, J. D., Schindler, K., & Pollefeys, M. (2017). SEMANTIC3D.NET: A new large-scale point cloud classification benchmark. *ISPRS Annals of the Photogrammetry, Remote Sensing and Spatial Information Science*, *IV-1-W1*, 91–98.

Hamner, B., & Frasco, M. (2018). Metrics: Evaluation metrics for machine learning. R Package Version 0.1.4 [Computer software] https://CRAN.R-project.org/package=Metrics

Heres, P., Rios, P., Cristobo, J., Abad-Uribarren, A., Rodríguez-Basalo, A., & Prado, E. (2024). Characterization of deep-sea sponge ground (*Asconema setubalense*) using structure from motion methodology. *Journal of Sea Research*, *200*, 102511. https://doi.org/10.1016/j.seares.2024.102511

Hess, C., Härdtle, W., Kunz, M., Fichtner, A., & von Oheimb, G. (2018). A high-resolution approach for the spatiotemporal analysis of forest canopy space using terrestrial laser scanning data. *Ecology and Evolution*, *8*(13), 6800–6811. https://doi.org/10.1002/ece3.4193

Innes, J. L. (1993). Methods to estimate forest health. *Silva Fennica*, *27*(2), 5507. https://www.silvafennica.fi/article/5507

Jacobsen, N. L., Roveta, C., Pulido Mantas, T., Coppari, M., Di Camillo, C. G., Calcinai, B., & Cerrano, C. (2024). Assessment of Octocoral-dominated benthic assemblages along a mesophotic gradient, with a focus on the impact of lost fishing gears. *Aquatic Conservation: Marine and Freshwater Ecosystems*, *34*(9), e4248. https://doi.org/10.1002/aqc.4248

Khosravipour, A., Skidmore, A. K., Wang, T., Isenburg, M., & Khoshelham, K. (2015). Effect of slope on treetop detection using a LiDAR canopy height model. *ISPRS Journal of Photogrammetry and Remote Sensing*, *104*, 44–52. https://doi.org/10.1016/j.isprsjprs.2015.02.013

Kuang, W., Ho, H. W., Zhou, Y., Suandi, S. A., & Ismail, F. (2024). A comprehensive review on tree detection methods using point cloud and aerial imagery from unmanned aerial vehicles. *Computers and Electronics in Agriculture*, *227*, 109476. https://doi.org/10.1016/j.compag.2024.109476

Küster, H. (2010). *Geschichte der Landschaft in Mitteleuropa: Von der Eiszeit bis zur Gegenwart*. C.H. Beck.

LaRue, E. A., Fahey, R., Fuson, T. L., Foster, J. R., Matthes, J. H., Krause, K., & Hardiman, B. S. (2022). Evaluating the sensitivity of forest structural diversity characterization to LiDAR point density. *Ecosphere*, *13*(9), e4209. https://doi.org/10.1002/ecs2.4209

Lasker, H. R., Bramanti, L., Edmunds, P. J., Girard, J. F., Pages, N., Tonra, K. J., Wells, C. D., & Guizien, K. (2025). Caribbean octocoral communities: Finding the forest for the trees? *Coral Reefs*. https://doi.org/10.1007/s00338-025-02692-z

Lasker, H. R., Bramanti, L., Tsounis, G., & Edmunds, P. J. (2020). The rise of octocoral forests on Caribbean reefs. In I. B. M. Riegl (Ed.), *Advances in marine biology* (Vol. *87*, Issue 1, pp. 361–410). Academic Press. https://doi.org/10.1016/bs.amb.2020.08.009

Li, Q., Zhang, X., Hao, D., Yan, W., Zhao, Q., Tian, Y., & Zeng, Y. (2025). Mapping tree height in complex terrain of northern China using ultra-high-resolution images. *Smart Agricultural Technology*, *12*, 101338. https://doi.org/10.1016/j.atech.2025.101338

Li, W., Hu, X., Su, Y., Tao, S., Ma, Q., & Guo, Q. (2024). A new method for voxel-based modelling of three-dimensional forest scenes with integration of terrestrial and airborne LiDAR data. *Methods in Ecology and Evolution*, *15*(3), 569–582. https://doi.org/10.1111/2041-210X.14290

Lin, Z., Shangguan, M., Cao, F., Yang, Z., Qiu, Y., Weng, Z., Lin, Z., Shangguan, M., Cao, F., Yang, Z., Qiu, Y., & Weng, Z. (2023). Underwater single-photon Lidar equipped with high-sampling-rate Multi-Channel data acquisition system. *Remote Sensing*, *15*(21), 5216. https://doi.org/10.3390/rs15215216

Liu, H., Zhong, H., Lin, W., & Wu, J. (2024). Tree species classification based on PointNet++ deep learning and true- colour point cloud. *International Journal of Remote Sensing*, *45*(16), 5577–5604. https://doi.org/10.1080/01431161.2024.2377837

Ma, Z., Dong, Y., Zi, J., Xu, F., Chen, F., Ma, Z., Dong, Y., Zi, J., Xu, F., & Chen, F. (2023). Forest-PointNet: A deep learning model for vertical

structure segmentation in complex Forest scenes. *Remote Sensing*, *15*(19), 4793. https://doi.org/10.3390/rs15194793

Manes, F., Marando, F., Capotorti, G., Blasi, C., Salvatori, E., Fusaro, L., Ciancarella, L., Mircea, M., Marchetti, M., Chirici, G., & Munafò, M. (2016). Regulating ecosystem services of forests in ten Italian metropolitan cities: Air quality improvement by PM10 and O_3 removal. *Ecological Indicators*, *67*, 425–440. https://doi.org/10.1016/j.ecolind.2016.03.009

Marlow, J., Halpin, J. E., & Wilding, T. A. (2024). 3D photogrammetry and deep-learning deliver accurate estimates of epibenthic biomass. *Methods in Ecology and Evolution*, *15*(5), 965–977. https://doi.org/10.1111/2041-210X.14313

Martínez-Quintana, Á., Lasker, H. R., & Wilson, A. M. (2023). Three-dimensional species distribution modelling reveals the realized spatial niche for coral recruitment on contemporary Caribbean reefs. *Ecology Letters*, *26*(9), 1497–1509. https://doi.org/10.1111/ele.14281

Meng, X., Currit, N., Zhao, K., Meng, X., Currit, N., & Zhao, K. (2010). Ground filtering algorithms for airborne LiDAR data: A review of critical issues. *Remote Sensing*, *2*(3), 833–860. https://doi.org/10.3390/rs2030833

Mielcarek, M., Stereńczak, K., & Khosravipour, A. (2018). Testing and evaluating different LiDAR-derived canopy height model generation methods for tree height estimation. *International Journal of Applied Earth Observation and Geoinformation*, *71*, 132–143. https://doi.org/10.1016/j.jag.2018.05.002

Munguia, P., & Ojanguren, A. F. (2015). Bridging the gap in marine and terrestrial studies. *Ecosphere*, *6*(2), 1–4. https://doi.org/10.1890/ES14-00231.1

Orejas, C., Carreiro-Silva, M., Mohn, C., Reimer, J., Samaai, T., Allcock, A. L., & Rossi, S. (2022). Marine animal forests of the world: Definition and characteristics. *Research Ideas & Outcomes*, *8*, e96274. https://doi.org/10.3897/rio.8.e96274

Palma, M., Magliozzi, C., Rivas Casado, M., Pantaleo, U., Fernandes, J., Coro, G., Cerrano, C., & Leinster, P. (2019). Quantifying coral reef composition of recreational diving sites: A structure from motion approach at seascape scale. *Remote Sensing*, *11*(24), 3027. https://doi.org/10.3390/rs11243027

Palma, M., Rivas Casado, M., Pantaleo, U., & Cerrano, C. (2017). High resolution Orthomosaics of African coral reefs: A tool for wide-scale benthic monitoring. *Remote Sensing*, *9*(7), 705. https://doi.org/10.3390/rs9070705

Palma, M., Rivas Casado, M., Pantaleo, U., Pavoni, G., Pica, D., & Cerrano, C. (2018). SfM-based method to assess gorgonian forests (*Paramuricea clavata* (Cnidaria, Octocorallia)). *Remote Sensing*, *10*(7), 1154. https://doi.org/10.3390/rs10071154

Pica, D., Calcinai, B., Poliseno, A., Trainito, E., & Cerrano, C. (2018). Distribution and phenotypic variability of the Mediterranean gorgonian *Paramuricea macrospina* (Cnidaria: Octocorallia). *The European Zoological Journal*, *85*(1), 392–408. https://doi.org/10.1080/24750263.2018.1529202

Ponti, M., Turicchia, E., Ferro, F., Cerrano, C., & Abbiati, M. (2018). The understorey of gorgonian forests in mesophotic temperate reefs. *Aquatic Conservation: Marine and Freshwater Ecosystems*, *28*(5), 1153–1166. https://doi.org/10.1002/aqc.2928

Popescu, S. C., & Wynne, R. H. (2004). Seeing the trees in the Forest. *Photogrammetric Engineering & Remote Sensing*, *70*(5), 589–604. https://doi.org/10.14358/PERS.70.5.589

Prado, E., Cristobo, J., Rodríguez-Basalo, A., Ríos, P., Rodríguez-Cabello, C., & Sánchez, F. (2021). In situ growth rate assessment of the Hexactinellid sponge *Asconema setubalense* using 3D photogrammetric reconstruction. *Frontiers in Marine Science*, *8*, 612613. https://doi.org/10.3389/fmars.2021.612613

Prado, E., Sánchez, F., Rodríguez-Basalo, A., Altuna, Á., & Cobo, A. (2019). Analysis of the population structure of a gorgonian forest (*Placogorgia* sp.) using a photogrammetric 3D modeling approach at Le Danois Bank, Cantabrian Sea. *Deep Sea Research. Part I, Oceanographic Research Papers*, *153*, 103124. https://doi.org/10.1016/j.dsr.2019.103124

Pulido Mantas, T., Roveta, C., Calcinai, B., Benelli, F., Coppari, M., Di Camillo, C. G., Pantaleo, U., Puce, S., & Cerrano, C. (2024). Structure from motion photogrammetry as an effective nondestructive technique to monitor morphological plasticity in benthic organisms: The case study of *Sarcotragus foetidus* Schmidt, 1862 (Porifera, Demospongiae) in the Portofino MPA. *Diversity*, *16*(3), 3. https://doi.org/10.3390/d16030175

Pulido Mantas, T., Roveta, C., Calcinai, B., Coppari, M., Di Camillo, C. G., Marchesi, V., Marrocco, T., Puce, S., & Cerrano, C. (2023). Photogrammetry as a promising tool to unveil marine caves' benthic assemblages. *Scientific Reports*, *13*(1), 7587. https://doi.org/10.1038/s41598-023-34706-7

Pulido Mantas, T., Roveta, C., Calcinai, B., di Camillo, C. G., Gambardella, C., Gregorin, C., Coppari, M., Marrocco, T., Puce, S., Riccardi, A., & Cerrano, C. (2023). Photogrammetry, from the land to the sea and beyond: A unifying approach to study terrestrial and marine environments. *Journal of Marine Science and Engineering*, *11*(4), 4. https://doi.org/10.3390/jmse11040759

Pulido Mantas, T., Roveta, C., Coppari, M., Di Camillo, C. G., Garrabou, J., Jacobsen, N. L., Palma, M., Pantaleo, U., Hendawitharana, M. P., & Cerrano, C. (2026). 3D point clouds and R code for the paper "As above, so below: A perspective into the application of land-forest monitoring methods for the assessment of marine animal forests" (No. Zenodo) [Dataset]. https://doi.org/10.5281/zenodo.18155450

Puliti, S., Dash, J. P., Watt, M. S., Breidenbach, J., & Pearse, G. D. (2020). A comparison of UAV laser scanning, photogrammetry and airborne laser scanning for precision inventory of small-forest properties. *Forestry: An International Journal of Forest Research*, *93*(1), 150–162. https://doi.org/10.1093/forestry/cpz057

R Core Team. (2024). *R: A language and environment for statistical computing*. R Foundation for Statistical Computing.

Rees, J. T. (1972). The effect of current on growth form in an octocoral. *Journal of Experimental Marine Biology and Ecology*, *10*(2), 115–123. https://doi.org/10.1016/0022-0981(72)90097-4

Remmers, T., Boutros, N., Wyatt, M., Gordon, S., Toor, M., Roelfsema, C., Fabricius, K., Grech, A., Lechene, M., & Ferrari, R. (2024). RapidBenthos: Automated segmentation and multi-view classification of coral reef communities from photogrammetric reconstruction. *Methods in Ecology and Evolution*, *16*(2), 427–441. https://doi.org/10.1111/2041-210X.14477

Riedl, R., & Forstner, H. (1968). Wasserbewegung im mikrobereich des benthos. *Sarsia*, *34*(1), 163–188. https://doi.org/10.1080/00364827.1968.10413380

Ríos, P., Prado, E., Carvalho, F. C., Sánchez, F., Rodríguez-Basalo, A., Xavier, J. R., Ibarrola, T. P., & Cristobo, J. (2020). Community composition and habitat characterization of a rock sponge aggregation (Porifera, Corallistidae) in the Cantabrian Sea. *Frontiers in Marine Science*, *7*, 578. https://doi.org/10.3389/fmars.2020.00578

Rossi, P., Ponti, M., Righi, S., Castagnetti, C., Simonini, R., Mancini, F., Agrafiotis, P., Bassani, L., Bruno, F., Cerrano, C., Cignoni, P., Corsini, M., Drap, P., Dubbini, M., Garrabou, J., Gori, A., Gracias, N., Ledoux, J.-B., Linares, C., & Capra, A. (2021). Needs and gaps in optical underwater technologies and methods for the investigation of marine animal Forest 3D-structural complexity. *Frontiers in Marine Science*, *8*, *591292*. https://doi.org/10.3389/fmars.2021.591292

Rossi, S. (2013). The destruction of the 'animal forests' in the oceans: Towards an over-simplification of the benthic ecosystems. *Ocean*

and Coastal Management, *84*, 77–85. https://doi.org/10.1016/j.ocecoaman.2013.07.004

Rossi, S., Bramanti, L., Gori, A., Orejas, C., Rossi, S., Bramanti, L., Gori, A., & Orejas, C. (2017). An overview of the animal forests of the world. In S. Rossi, L. Bramanti, A. Gori & C. Orejas (Eds.), *Marine animal forests. The ecology of benthic biodiversity hotspots* (pp. 1–26). https://doi.org/10.1007/978-3-319-17001-5_1-11007/978-3-319-17001-5_1-1

Rossi, S., Bramanti, L., Horta, P., Allcock, L., Carreiro-Silva, M., Coppari, M., Denis, V., Hadjioannou, L., Isla, E., Jimenez, C., Johnson, M., Mohn, C., Orejas, C., Ramšak, A., Reimer, J., Rinkevich, B., Rizzo, L., Salomidi, M., Samaai, T., & Zorrilla-Pujana, J. (2022). Protecting global marine animal forests. *Science*, *376*(6596), 929. https://doi.org/10.1126/science.abq7583

Roussel, J.-R., Auty, D., Coops, N. C., Tompalski, P., Goodbody, T. R. H., Meador, A. S., Bourdon, J.-F., de Boissieu, F., & Achim, A. (2020). lidR: An R package for analysis of airborne laser scanning (ALS) data. *Remote Sensing of Environment*, *251*, 112061. https://doi.org/10.1016/j.rse.2020.112061

Rusu, R. B., & Cousins, S. (2011). *3D is here: Point cloud library* (*PCL*), 1–4 https://doi.org/10.1109/ICRA.2011.5980567

Sacchelli, S., Borghi, C., Fratini, R., Bernetti, I., Sacchelli, S., Borghi, C., Fratini, R., & Bernetti, I. (2021). Assessment and valorization of non-wood forest products in Europe: A quantitative literature review. *Sustainability*, *13*(6), 3533. https://doi.org/10.3390/su13063533

Saeed, T., Hussain, E., Ullah, S., Iqbal, J., Atif, S., & Yousaf, M. (2024). Performance evaluation of individual tree detection and segmentation algorithms using ALS data in Chir pine (*Pinus roxburghii*) forest. *Remote Sensing Applications: Society and Environment*, *34*, 101178. https://doi.org/10.1016/j.rsase.2024.101178

Sannigrahi, S., Chakraborti, S., Joshi, P. K., Keesstra, S., Sen, S., Paul, S. K., Kreuter, U., Sutton, P. C., Jha, S., & Dang, K. B. (2019). Ecosystem service value assessment of a natural reserve region for strengthening protection and conservation. *Journal of Environmental Management*, *244*, 208–227. https://doi.org/10.1016/j.jenvman.2019.04.095

Sauder, J., Banc-Prandi, G., Meibom, A., & Tuia, D. (2024). Scalable semantic 3D mapping of coral reefs with deep learning. *Methods in Ecology and Evolution*, *15*(5), 916–934. https://doi.org/10.1111/2041-210X.14307

Smeds, E. A., Cooper, Z., & Bentley, L. P. (2025). Lacunr: Efficient 3D lacunarity for voxelized LiDAR data from forested ecosystems. *Methods in Ecology and Evolution*, *16*(9), 1906–1913. https://doi.org/10.1111/2041-210X.70126

Smith, H. A., Boström-Einarsson, L., & Bourne, D. G. (2022). A stratified transect approach captures reef complexity with canopy-forming organisms. *Coral Reefs*, *41*(4), 897–905. https://doi.org/10.1007/s00338-022-02262-7

Torres-Pulliza, D., Dornelas, M. A., Pizarro, O., Bewley, M., Blowes, S. A., Boutros, N., Brambilla, V., Chase, T. J., Frank, G., Friedman, A., Hoogenboom, M. O., Williams, S., Zawada, K. J. A., & Madin, J. S. (2020). A geometric basis for surface habitat complexity and biodiversity. *Nature Ecology & Evolution*, *4*(11), 1495–1501. https://doi.org/10.1038/s41559-020-1281-8

Tsounis, G., Edmunds, P. J., Bramanti, L., Gambrel, B., & Lasker, H. R. (2018). Variability of size structure and species composition in Caribbean octocoral communities under contrasting environmental conditions. *Marine Biology*, *165*(2), 29. https://doi.org/10.1007/s00227-018-3286-2

Turner, J. A., Babcock, R. C., Hovey, R., & Kendrick, G. A. (2017). Deep thinking: A systematic review of mesophotic coral ecosystems. *ICES Journal of Marine Science*, *74*(9), 2309–2320. https://doi.org/10.1093/icesjms/fsx085

Urbina-Barreto, I., Chiroleu, F., Pinel, R., Fréchon, L., Mahamadaly, V., Elise, S., Kulbicki, M., Quod, J.-P., Dutrieux, E., Garnier, R., Henrich Bruggemann, J., Penin, L., & Adjeroud, M. (2021). Quantifying the shelter capacity of coral reefs using photogrammetric 3D modeling: From colonies to reefscapes. *Ecological Indicators*, *121*, 107151. https://doi.org/10.1016/j.ecolind.2020.107151

Urbina-Barreto, I., Garnier, R., Elise, S., Pinel, R., Dumas, P., Mahamadaly, V., Facon, M., Bureau, S., Peignon, C., Quod, J.-P., Dutrieux, E., Penin, L., & Adjeroud, M. (2021). Which method for which purpose? A comparison of line intercept transect and underwater photogrammetry methods for coral reef surveys. *Frontiers in Marine Science*, *8*, 636902. https://doi.org/10.3389/fmars.2021.636902

Webb, T. J. (2012). Marine and terrestrial ecology: Unifying concepts, revealing differences. *Trends in Ecology & Evolution*, *27*(10), 535–541. https://doi.org/10.1016/j.tree.2012.06.002

Weimbauer, M. G., & Velimirov, B. (1998). Comparative morphometry of fan-like colonies of three Mediterranean gorgonians (Cnidaria: Gorgonacea). *Cahiers de Biologie Marine*, *39*, 41–49.

Weinberg, S. (1976). Revision of the common Octocorallia of the Mediterranean circalittoral. I. Gorgonacea. *Beaufortia*, *313*, 63–103.

Weiser, H., Winiwarter, L., Anders, K., Fassnacht, F. E., & Höfle, B. (2021). Opaque voxel-based tree models for virtual laser scanning in forestry applications. *Remote Sensing of Environment*, *265*, 112641. https://doi.org/10.1016/j.rse.2021.112641

Wu, S., Chen, C., Yang, B., Yan, Z., Wang, Z., Sun, S., Zou, Q., & Fu, J. (2025). PylonModeler: A hybrid-driven 3D reconstruction method for power transmission pylons from LiDAR point clouds. *ISPRS Journal of Photogrammetry and Remote Sensing*, *220*, 100–124. https://doi.org/10.1016/j.isprsjprs.2024.12.003

Zentner, Y., Rovira, G., Margarit, N., Ortega, J., Casals, D., Medrano, A., Pagès-Escolà, M., Aspillaga, E., Capdevila, P., Figuerola-Ferrando, L., Riera, J. L., Hereu, B., Garrabou, J., & Linares, C. (2023). Marine protected areas in a changing ocean: Adaptive management can mitigate the synergistic effects of local and climate change impacts. *Biological Conservation*, *282*, 110048. https://doi.org/10.1016/j.biocon.2023.110048

Zhang, H., Wang, C., Tian, S., Lu, B., Zhang, L., Ning, X., & Bai, X. (2023). Deep learning-based 3D point cloud classification: A systematic survey and outlook. *Displays*, *79*, 102456. https://doi.org/10.1016/j.displa.2023.102456

Zhang, W., Qi, J., Wan, P., Wang, H., Xie, D., Wang, X., & Yan, G. (2016). An easy-to-use airborne LiDAR data filtering method based on cloth simulation. *Remote Sensing*, *8*(6), 6. https://doi.org/10.3390/rs8060501

Zhang, Y., Liu, Y., Liu, Q., Zhang, X., Huang, C., Li, H., Peng, Y., & Liu, B. (2025). Individual tree detection from aerial RGB images using transfer learning semantic segmentation and simulated illumination template matching in the Yellow River Delta. *Science of Remote Sensing*, *12*, 100313. https://doi.org/10.1016/j.srs.2025.100313

Zong, X., Wang, T., Skidmore, A. K., & Heurich, M. (2021). The impact of voxel size, forest type, and understory cover on visibility estimation in forests using terrestrial laser scanning. *GIScience & Remote Sensing*, *58*(3), 323–339. https://doi.org/10.1080/15481603.2021.1873588

SUPPORTING INFORMATION

Additional supporting information can be found online in the Supporting Information section at the end of this article.

File S1. R Markdown containing the commented R code to implement the proposed pipeline to process Marine Animal Forest's point clouds.

Table S1. Summary of site information (depth, assessed surface, sampling date), camera systems used, imagery.

Table S2. Sensitivity analysis results for main processing steps of the proposed point cloud classification pipeline. Please note: Parameter combinations yielding results most consistent with visual inspection and/or manual methods are highlighted in green.

Table S3. Summary of point density calculation results at 10 cm × 10 cm patch for all study sites.

Figure S1. Image composite of point density maps calculated at 10 cm × 10 cm patch: (a) Punta del Faro, (b).

How to cite this article: Pulido Mantas, T., Roveta, C., Coppari, M., Di Camillo, C. G., Garrabou, J., Jacobsen, N. L., Palma, M., Pantaleo, U., Hendawitharana, M. P., & Cerrano, C. (2026). As above, so below: A perspective into the application of land-forest monitoring methods for the assessment of marine animal forests. *Methods in Ecology and Evolution*, *17*, 1124–1142. https://doi.org/10.1111/2041-210x.70242